Direct impact of gonadotropins on glucose uptake and storage in preovulatory granulosa cells: Implications in the pathogenesis of polycystic ovary syndrome

Nidhi Chahal, Anjali Geethadevi, Surleen Kaur, Ruchi Lakra, Anjali Nagendra, Tulsidas G. Shrivastav, Francesco de Pascali, Eric Reiter, Pascale Crépieux, M. Gouri Devi, et al.

Direct impact of gonadotropins on glucose uptake and storage in preovulatory granulosa cells: Implications in the pathogenesis of polycystic ovary syndrome

Nidhi Chahal, Anjali Geethadevi, Surleen Kaur, Ruchi Lakra, Anjali Nagendra, T G Shrivastav, Francesco de Pascali, Eric Reiter, Pascale Crépieux, M Gouri Devi, et al.

Direct impact of gonadotropins on glucose uptake and storage

Nidhi Chahal, Anjali Geethadevi, Surleen Kaur, Ruchi Lakra, Anjali Nagendra, T.G. Shrivastav, Francesco De Pascali, Eric Reiter, Pascale Crépieux, M. Gouri Devi, Neena Malhotra, K. Muralidhar, Rita Singh

PII: S0026-0495(20)30322-X

DOI: https://doi.org/10.1016/j.metabol.2020.154458

Reference: YMETA 154458

To appear in: *Metabolism*

Received date: 12 August 2020

Accepted date: 27 November 2020

Please cite this article as: N. Chahal, A. Geethadevi, S. Kaur, et al., Direct impact of gonadotropins on glucose uptake and storage, *Metabolism* (2020), https://doi.org/10.1016/j.metabol.2020.154458

Direct impact of gonadotropins on glucose uptake and storage in preovulatory granulosa cells: Implications in the pathogenesis of polycystic ovary syndrome

[*a]Nidhi Chahal, [*a,b]Anjali Geethadevi, [a,c]Surleen Kaur, [a]Ruchi Lakra, [a]Anjali Nagendra, [d]T.G. Shrivastav, [e]Francesco De Pascali, [e]Eric Reiter, [e]Pascale Crépieux, [f]M. Gouri Devi, [g]Neena Malhotra, [a]K. Muralidhar, [a,†]Rita Singh,

[a]Division of Molecular Endocrinology and Reproduction, Department of Zoology, University of Delhi, Delhi, India; [b]Medical College of Wisconsin, Milwaukee 53226, USA; [c]Ferticity Fertility Clinics, Delhi, India; [d]National Institute of Health and Family Welfare, Delhi, India; [e]Physiologie de la Reproduction et des Comportements, INRAE UMR-0085, CNRS UMR-7247, Université de Tours, IFCE, F-37380 Nouzilly, France; [f]Gouri Hospitals, Malka Ganj, Delhi, India; [g]Department of Obstetrics and Gynecology, All India Institute of Medical Sciences, Delhi, India.

*Both authors have contributed equally

Running Title: Direct impact of gonadotropins on glucose uptake and storage

†Corresponding Author

Address: Prof. Rita Singh, Division of Molecular Endocrinology and Reproduction
Department of Zoology, University of Delhi, Delhi 110007, India
Telephone: +91-8527820707, 91-11-27666466
E-mail: ghrika_s@yahoo.com, ritas@zoology.du.ac.in

Abbreviations: FSH, Follicle stimulating hormone; hCG, Human chorionic gonadotropin; LH, Luteinizing hormone; PI3K, Phosphoinositide 3-kinase; IRS-2, Insulin receptor substrate-2; GCs, Granulosa cells; PCOS, Polycystic ovary syndrome; GS, Glycogen synthase; Akt, Protein kinase B; PCOS-IR, PCOS with insulin resistance; PCOS non-IR, PCOS without insulin resistance; RTKs, Receptor tyrosine kinase; GPCR, G-protein coupled receptors, LHR, Luteinizing hormone receptor; FSHR, FSH receptor; InsR, Insulin receptor; IGF-1R, IGF-1 receptor.

Abstract

Background: Polycystic ovary syndrome (PCOS) is often associated with higher levels of LH, and arrested ovarian follicular growth. The direct impact of high LH on FSH mediated metabolic responses in PCOS patients is not clearly understood.

Method: In order to investigate the impact of FSH and LH on glucose metabolism in preovulatory granulosa cells (GCs), we used [U-^{14}C]-2 deoxyglucose, D-[U-^{14}C]-glucose or 2-NBD glucose to analyse glucose uptake and its incorporation into glycogen. To reproduce the high androgenic potential in PCOS patients, we administered hCG both *in vitro* and *in vivo*. The role of IRS-2/PI3K/Akt2 pathway was studied after knockdown with specific siRNA. Immunoprecipitation and specific assays were used for the assessment of IRS-2, glycogen synthase and protein phosphatase 1. Furthermore, we examined the *in vivo* effects of hCG on FSH mediated glycogen increase in normal and PCOS rat model. HEK293 cells co-expressing FSHR and LHR were used to demonstrate glucose uptake and BRET change by FSH and hCG.

Results: In normal human and rat granulosa cells, FSH is more potent than hCG in stimulating glucose uptake, however glycogen synthesis was significantly upregulated only by FSH through increase in activity of glycogen synthase via IRS-2/PI3K/Akt2 pathway. On the contrary, an impaired FSH-stimulated glucose uptake and glycogen synthesis in granulosa cells of PCOS-patients indicated a selective defect in FSHR activation. Further, in normal human granulosa cells, and in immature rat model, the impact of hCG on FSH response was such that it inhibited the FSH-mediated glucose uptake as well as glycogen synthesis through inhibition of FSH-stimulated IRS-2 expression. These findings were further validated in HEK293 cells overexpressing Flag-LHR and HA-FSHR, where high hCG inhibited the FSH-stimulated glucose uptake. Notably, an increased BRET change was observed in HEK293 cells expressing FSHR-Rluc8 and LHR-Venus possibly suggesting increased heteromerization of LHR and FSHR in the presence of both hCG and FSH in comparison to FSH or hCG alone.

Conclusion: Our findings confirm a selective attenuation of metabolic responses to FSH such as glucose uptake and glycogen synthesis by high activation level of LHR leading to the inhibition of IRS-2 pathway, resulting in depleted glycogen stores and follicular growth arrest in PCOS patients.

Keywords: FSH, LH, Granulosa cells, PCOS, IRS-2, Glucose, Glycogen, Metabolism.

1. Introduction

Polycystic ovary syndrome (PCOS) is one of the most common endocrinopathies leading to subfertility or infertility in women of reproductive age [1-2]. PCOS women are more susceptible to develop metabolic abnormalities such as insulin resistance [1,3-4]. In PCOS women, the ovarian follicular growth is disordered as it gets arrested at mid-antral stage [5]. Most PCOS women have an abnormal *ratio* of luteinizing hormone (LH) and follicle stimulating hormone (FSH), due to higher basal level and increased pulse frequency of LH [6-7]. Several hypotheses have emerged as to how LH hypersecretion may adversely affect follicular growth and differentiation in PCOS patients. These hypotheses were substantiated by transgenic mice model where over-expression of LH or hCG resulted in polycystic ovaries and infertility [8-9]. The most popular hypothesis states that increased steroidogenesis and hyperandrogenism due to high LH level contribute to PCOS development [2]. An elevated LH may also dysregulate follicular development by decreasing FSH sensitivity [10]. Most studies showed a normal to exaggerated serum E_2-responsiveness to FSH in normal-weight PCOS women [11].

Granulosa cells (GCs) and oocytes have metabolic cooperation for the continuous supply of glucose and any alteration in this process may have deleterious effects on follicular growth and oocyte maturation. Both FSH and LH stimulate glucose uptake as demonstrated in oocyte-cumulus cell complexes [12] and GCs [13]. However, the relative difference in the potency of FSH and LH for glucose uptake in preovulatory GCs is not known. Previous studies have established that LH is more glycolytic than FSH [12]. Further, the metabolic fate of FSH-stimulated glucose uptake in preovulatory GCs is not clearly known. Earlier, accumulation of glycogen has been observed in ovarian follicles especially in GCs of antral and preovulatory ovine follicles 48h before ovulation [14-15]. However, little is known about the relative role of FSH and LH in the regulation of glycogen levels in preovulatory follicles. Intriguingly, the impact of high LH on the metabolic responses of FSH, which may contribute to PCOS condition, is also not clear.

Glycogen synthesis is primarily known to be stimulated by insulin in peripheral tissues as well as in ovaries [16]. The molecular mechanisms by which the enzymatic effectors involved in glycogenesis are regulated in preovulatory follicles remain poorly understood. FSH and insulin have overlapping effects on the signaling cascades to increase glucose uptake via translocation of glucose transporter 4 (GLUT4) to the plasma membrane and the activation of hexokinase [16-17].

Both FSH and LH bind to their specific G protein-coupled receptors and activate the classical cAMP/protein kinase A (PKA) pathway in addition to several other signaling pathways such as IRS-2/PI3K/Akt2 and MAPK pathways [17-18]. LH receptor (LHR) binds both pituitary-derived LH and the placental hormone, chorionic gonadotropin (hCG), while the FSH receptor (FSHR) only binds the pituitary-derived FSH. LHR gets constitutively expressed on theca and interstitial cells whereas its

expression is regulated by FSH in preovulatory GCs [19-20]. FSHR expression starts in GCs of early follicles, whereas LHR expression becomes prominent just prior to ovulation (preovulatory stage) and luteinizing follicles. Once acquired FSHR remains on GCs of healthy follicles until they become atretic or luteinize. In PCOS follicles, GCs have premature and higher expression of LHR whereas the expression of FSHR is either normal or higher [21]. No change in the expression of insulin receptor (InsR) has been observed and the expression of IGF-1 receptor (IGF-1R) is normal in PCOS GCs [5,10, 22].

Earlier, we had shown that FSH increases IRS-2 expression, which is crucial for PI3K-Akt2-mediated translocation of GLUT4 to cell membrane and consequent uptake of glucose in preovulatory rat GCs [17]. FSH-stimulated increase in IRS-2 which is an early step in the cross-talk between FSH and insulin/IGF-1 pathways was impaired in PCOS GCs [17]. Previous studies indicate that IRS-2-deleted mice are infertile and resistant to the exogenous gonadotropins [23-24]. However, InsR knockout mice have normal fertility and litter size [25]. Therefore, we hypothesized that FSH signaling could cross-talk with insulin signaling pathway through IRS-2 and a defect in this pathway could be responsible for impaired metabolism in PCOS patients and poor fertility outcome.

Here, we assessed the impact of LH on FSH-regulated metabolic responses in physiological conditions as well as in PCOS patients. Our findings suggest that abnormal LH levels may selectively attenuate the metabolic responses of FSH such as glucose uptake and its storage as glycogen in GCs. Our findings reported here will help in exploring new therapies and therapeutic targets for women with PCOS in future.

2. Materials and Methods

2.1 Materials:

The materials used in this study can be found in supplemental materials and in our previous publications [3, 17].

2.2 Subjects:

Following the approval by institutional ethics committees (IEC/NP-293/2012-RF-16/2013; IHEC/DU/NP-2/2012; IHEC/DU/NP-1/2018), we enrolled PCOS women with or without insulin resistance as per Rotterdam criteria as described earlier [3,17, 26]. The details of the subjects contributing to this study are given in Supplemental Table 1. General inclusion criteria for all participants were age less than 35 years, normal prolactin levels, and normal thyroid function [3, 17]. The selection criteria for control women were as follows: regular menstrual cycles occurring every 25–35 d, no clinical or biochemical evidence of hyperandrogenism, no polycystic ovaries, and without insulin resistance. These women were receiving assisted reproduction for non-ovarian indications, such as male or tubal factor infertility. PCOS patients did not receive clomiphene citrate or antidiabetic drugs during stimulation cycles. All methods performed are in accordance with the relevant guidelines and regulations. We collected the ovarian aspirates of 41 non-hirsute ovulatory women and 61 PCOS women with or without insulin resistance, after the gonadotropin therapy for *in vitro* fertilization (IVF). Insulin resistance in PCOS was assessed by calculating the homeostasis model assessment (HOMA-IR) index and 2.5 was selected as a cutoff point [3, 17].

2.3 Granulosa cell culture and treatments

We isolated the human GCs from the follicular fluid aspirates obtained after the IVF therapy of normal and PCOS women as described earlier [17]. The cells were suspended in complete media, Dulbecco's Modified Eagle's medium (DMEM) containing 5% foetal bovine serum (FBS, cat # RM9955, South American origin, EU approved), antibiotic and antimycotic solution (Himedia Biosciences, India), and cultured in 5% CO_2 at 37 °C (Thermo Scientific, USA).

The animal experiments were performed under the guidance of institutional animal ethics committee (DU/2001/IAEC-R/2013/37). Twenty-six day old immature female rats (Holtzman strain, Total=42) were primed with pregnant mare serum gonadotropin (PMSG, 10U/d for 3 d) and GCs were isolated from preovulatory follicles described earlier [17]. We used GCs cultured in DMEM supplemented with 10% FBS, antibiotic solution and grown to 70% confluency in 5% CO_2 at 37 °C.

Human or rat granulosa cells were cultured and serum starved on day 3 of culture for 16 h overnight and then treated with different concentrations of recombinant human FSH (10,000 U/mg protein, Recagon, Organon, Ireland), human chorionic gonadotropin (Urinary origin hCG, CG-10, 10,000 U/mg protein, Sigma-Aldrich, see details in Supplemental materials) or in combination for 1 h before

addition of [U-^{14}C]-2 deoxyglucose (1 µCi) or 2-(N-(7-Nitrobenz-2-oxa-1,3-diazol-4-yl) amino)-2-deoxyglucose (2-NBDG, 200µM) for 30 min for glucose uptake and 3h for glycogen synthesis. To reproduce the high androgenic potential in PCOS patients, we administered hCG both *in vitro* and *in vivo.* To compare the effect of FSH and hCG on glucose uptake, rat preovulatory GCs were treated with FSH alone or hCG alone and in combination for 1h before the addition of 2-NBDG for 30 min, *in vitro*.

To study FSH-mediated glycogen synthesis, GCs were also treated with LY294002 (PI3K inhibitor, 10 µM), Akt inhibitor IV (7 µM), phosphatase inhibitors- okadaic acid (OA, 50 nM) and calyculin A (Cal A, 5 nM), and D-[U-^{14}C]-glucose (specific activity, 150-250 mCi/mmole) 30 min before the FSH treatment.

To find out if the role of FSH in stimulating the glycogen synthesis in preovulatory GCs is Estradiol (E_2) mediated, we examined the glucose uptake and glycogen synthesis in rat preovulatory GCs in the presence of 3.3 nM FSH or 50 nM E_2 [27] or 4µg/ml anti-E_2, a non-steroidal compound, 2-[piperdinoethoxyphenyl]-3-[4-methoxyphenyl]-2H benzopyran (K-7) [28] or in combination of these for 1h before addition of 2-NBDG for 3h. Glycogen was extracted by KOH method and fluorescence was measured as described in the section 2.4.

The siRNA specific to Akt (Akt2), PI3K (p85α), IRS-2 and scrambled siRNA (Santa Cruz Biotechnology, USA), were transfected into GCs by using RNAiFect (Qiagen, Germany). The efficiency and specificity of each siRNA-mediated knockdown was monitored as described earlier [17].

2.4 Glycogen assay

Serum starved GCs were treated with FSH for 1h, [U-^{14}C]-2 deoxyglucose (1 µCi) or 2-NBDG (200 µM) was added to each well and further incubated for 3h [29]. The cells were homogenized in 30% KOH saturated with sodium sulphate, and the extracts were boiled for 30 min after addition of 2 mg carrier glycogen. Then, 2 volumes of 95% ethanol was added and glycogen was precipitated overnight at -20ºC. In these conditions, free glucose did not precipitate. Radioactivity was measured in the pellets with a liquid scintillation counter (Wallac 1450 MicroBeta® TriLux scintillation counter). The 2-NBDG-glycogen fluorescence in samples was measured in black 96-well plate (Greiner) using fluorescence plate reader (Fluostar® Optima, BMG Labtech GmbH (Ortenberg, Germany) at 480 nm excitation and 535 nm emission wavelengths. Protein content was measured in cell lysates by Bradford assay [17].

For confocal imaging of glycogen granules, control and FSH-treated GCs in 4-well slides (BD Biosciences) were fixed in 4% paraformaldehyde in 1X PBS for 10 min. After washing, the cells were mounted using Ultra Cruz mounting medium. Fluorescent images were observed with a 63x oil immersion objective of Leica TCS SP5 confocal microscope. The images were processed using LAS

AF Lite software (Leica Microsystems Inc. Germany). The quantification of relative mean optical intensity (ROI) was done using Image J software.

2.5 Estimation of glycogen in ovaries

Immature female rats (26 d old, total=45) were divided into seven groups based on the hormonal treatments. In the first experiment, these were: group 1. FSH (8 IU/d) treatment for one day (n=5), group 2. FSH (8 IU/d) treatment for two days (n=5), and group 3. FSH (8 IU/d) treatment for three days (n=10). group 4. Treatment with FSH (8 IU/day) for 3 days followed by hCG (10 IU/day) on 3rd day (n=5). group 5. Treatment with hCG alone (10 IU/day) for 3 days (n=5), group 6. A control group of immature female rats was treated with saline for respective duration (n=10). The animals were sacrificed at the end of treatments and ovaries were processed for glycogen extraction by KOH treatment, and estimation by phenol-sulphuric acid method [30].

2.6 Glycogen synthase (GS) activity

For determining the GS activity, serum starved GCs were treated with FSH for varying time periods. After washing with PBS, the cells were scraped and then sonicated in NaF-EDTA solution (2.5 mM EDTA, 10 mM NaF) for 10 secs and 100 µl of this extract was added to GS assay buffer (200 µl). To measure the activity of GS (in the absence of glucose-6-phosphate), a buffer containing 3 mM Uridine diphosphate glucose and UDP-[U-^{14}C] glucose (specific activity: 200 mCi/mmol) was added and then incubated for 20 min at 37°C. After overnight precipitation with ethanol (95%) at -20°C, samples were centrifuged and radioactivity was measured in the pellets using a liquid scintillation counter. The activity of GS in this assay was represented as nmoles of UDP-glucose incorporated per mg protein per hour.

2.7 Animal model of PCOS

Adult rats (3 months old) received subcutaneous (s.c.) injections (4 mg/0.2ml olive oil/d, n=6/group, Total=18) of RU486 (Sigma Chemicals, St. Louis, MO, USA) daily for 18 days beginning on the day of proestrus (Day 1 of the experiment) as described earlier [17]. After the treatment, the ovaries were processed for glycogen extraction and estimation as described above. The control ovaries were taken from rats that were in proestrus or oestrus stage after olive oil injection for 18 days.

2.8 Immunoprecipitation

Control, and FSH-treated GCs were harvested in 20 mM Tris-HCl pH 7.5, 150 mM NaCl, 0.5% sodium deoxycholate, 1% Triton X-100, 2 mM EDTA and the extracts were prepared by homogenization. Equal amount of protein was taken for each sample and to the precleared supernatant, 10 µl of IRS-2 antibody (Santa Cruz Biotechnology, USA) and protein-A agarose were added, and the mixture was kept for 15h at 4°C. Immune complexes were eluted from protein-A agarose and were subjected to Western blotting.

2.9 Western Blotting

Proteins extracted from GCs (50 µg), and the immune complexes obtained with IRS-2 antibody were fractionated on 10% and 7.5% SDS-PAGE respectively. The proteins were transferred onto nitrocellulose membranes which were then incubated for 2h at 25°C with either of the primary antibodies to p-GSK3β, GSK3β, p-Tyr, p-Ser or β-actin (Santa Cruz Biotechnology, USA). The Western blots were further incubated with appropriate horseradish peroxidase-conjugated secondary antibodies, anti-goat IgG-Cy3 and anti-rabbit IgG-Cy3 antibodies (Sigma Aldrich Chemicals Pvt Ltd, USA). Presence of bound antibodies was detected by enhanced chemiluminescence (ECL) reaction using the ECL Plus kit (Millipore, USA).

2.10 Immunofluorescence

Cultured cells were fixed with 4% paraformaldehyde for 10 min and permeabilized with 0.1% Triton-X 100. For studying the colocalization of GS with 2-NBDG, monolayer cultures of GCs in culture slides (BD Bioscience) were incubated with 2-NBDG (500 µM) after 1h incubation with FSH at a concentration of 3.3 nM equivalent approximately to EC_{50} of glycogen synthesis for 3h. After blocking with 5% BSA, the slides were incubated with 1:50 dilution of anti-GS-1 (mouse) antibody (Santa Cruz Biotechnology, USA) at 4°C overnight. GS exhibited red fluorescence from Cy3-conjugated anti-mouse secondary antibody (Santa Cruz Biotechnology, USA) and 2-NBDG, a green fluorescence while nuclei were counterstained with DAPI (4', 6-diamidino-2-phenylindole). The images were processed as described earlier. The quantification of signal overlap was determined using Pearson Correlation Coefficient (Leica LAS AF software).

2.11 RNA isolation and reverse-transcription quantitative PCR (qRT-PCR)

Total RNA was extracted using TRI reagent (Sigma) from rat GCs treated with FSH, hCG and FSH + hCG and untreated cells that were used as control. IRS-2 RNA was quantified by qPCR as described earlier [17]. The primers for IRS-2 and β2M were as follows:
IRS-2 (F) 5′-TCGGACACCTTCTTCTTCA-3′, (R) 5′-ATGGTCTCGTGGATGTTCT-3′,
β2M (F) 5′-TGCTCGCGCTACTCTCTCTT-3′, (R) 5′-TCAACTTCAATGTCGGATGG-3′.

2.12 Protein phosphatase 1 (PP1) assay

PP1 activity was determined by measuring the formation of DiFMU (6,8-Difluoro-7-Hydroxy-4-Methylcoumarin) from the substrate DiFMUP (6,8-Difluoro-4-Methylumbelliferyl Phosphate) at 37°C [31]. The cells were lysed in homogenization buffer and supernatants were incubated with PP1 antibody (Santa Cruz Biotechnology, USA) and the immune complexes were immobilized on protein A-agarose. After washing, the immune complexes immobilized on protein A-agarose were incubated at 37 °C for 1 h with PP1 assay buffer at pH 7.5. The reaction was initiated by the addition of 50 µM DiFMUP substrate. To study the signaling pathways involved in FSH-mediated increase in PP1

activity, GCs were also treated with PI3K inhibitor (LY294002, 10 µM), Akt inhibitor IV (7 µM), Phosphatase inhibitors-okadaic acid (OA, 20 nM) and calyculin A (Cal A, 0.5 nM), 30 min before the FSH treatment. Thereafter, the fluorescence was measured in the fluorescence plate reader (Fluostar Optima) at the excitation/emission wavelengths of 360 nm / 460 nm. For the measurement of total PP1 enzyme activity, a linear regression analysis was performed and its slope indicates phosphatase activity in relative fluorescence units per hour (RFU/h). The phosphates released were quantified by comparison of the measured RFUs with the fluorescence of DiFMU. A standard curve derived from the provided reference standards was used to convert the fluorescence units obtained in the assay into nanomoles (nmoles) of phosphate. One nmole of the included reference standard, DiFMU, is equivalent to one nmole of phosphate released by the cleavage of the substrate, DiFMUP. The results are represented as nmoles of phosphate released per mg protein per hour.

2.13 Measurement of glucose uptake in HEK293 cells expressing both LHR and FSHR

For transfections, plasmid DNA (50 ng/well) of HA-FSHR or FLAG-LHR was diluted in 25 µl/well DMEM without phenol red and FBS. Both plasmids and HEK293 cells were provided by Dr. Aylin Hanyaloglu (Imperial College London, London, UK). Transfection Reagent (ViaFect™ Promega, 0.5 µL/well) was mixed with 25 µl/ well of DMEM and the two solutions were mixed and incubated at room temperature for 20 min. HEK293 cells (80,000 cells/well) were added to the above solution in a 96-well plate and incubated at 37°C in 5% CO_2. After 48 hours, cells were serum-starved overnight. HEK293 cells expressing both FSHR and LHR were treated with different concentrations of FSH alone, hCG alone and FSH + hCG for 1h, followed by addition of 2-NBDG (200µM) for 30 min. The cells were washed with PBS and transferred to Greiner 96-well black plate. Fluorescence due to 2-NBDG uptake was measured using fluorescence plate reader (FLUOstar OPTIMA) at 480 nm excitation and 535 nm emission wavelength.

2.14 Bioluminescence Resonance Energy Transfer (BRET) measurement in HEK293 cells after co-transfection with FSHR-Luc8 and LHR-Venus

HEK293 cells were cultured for forty-eight hours before BRET measurement. HEK293 cells were co-transfected with the FSHR fused with the Renilla luciferase 8 BRET donor (FSHR-Luc8) and with LHR fused with the Venus BRET acceptor (LHR-Venus) using Metafectene Pro (Biontex Laboratories GmbH, Munich, Germany). Both plasmids were provided by Dr. Aylin Hanyaloglu (Imperial College London, London, UK). The two transfection mixes (Mix A and B) were prepared and incubated separately for 5 min. Mix A contained 50 ng/well of FSHR-luc8 plus 120 ng/well of LHR-Venus diluted in 25 µl/well in DMEM. Mix B contained 0.5 µL/well of Metafectene Pro and 25 µl/ well of DMEM. The two solutions were mixed and incubated at room temperature for 20 min., then cells (80,000 cells/well) were added and cultured in opaque 96-well plates (Greiner Bio One International GmbH, Kremsmünster, Austria). After 48 hours, cells were starved overnight in a serum-

free medium. These cells in 30 µl/well of PBS without Ca^{2+} and Mg^{2+} were stimulated with increasing concentrations of FSH or hCG in 10 µl (FSH was a kind gift from Merck KGaA, Darmstadt, Germany; hCG was a kind gift from Dr. Y. Combarnous, CNRS, Nouzilly, France) and a fixed concentration of hCG or FSH in10 µl, respectively. Finally, 10 µl/well of Coelenterazine H, the Renilla luciferase substrate (Interchim, Montluçon, USA) was added to each well to a final concentration of 5 µM and the BRET signal was immediately detected and registered for 30 min by using a Mithras LB 943 plate reader (Berthold Technologies GmbH & Co., Wildbad, Germany). Results are expressed as area under the curve from 5 experiments and were analyzed by one way ANOVA.

2.15 Statistical analysis

Statistical significance of differences between two groups was determined by unpaired Student's t-test. One way ANOVA was applied to compare the data between the groups. [^{14}C]-Glycogen levels in GCs were converted from cpm to pmoles of glucose units incorporated per mg protein per hour. Incorporation of 2-NBDG into glycogen was expressed as relative fluorescence units (RFUs). Statistical analyses were performed using Prism Version 7.0a (GraphPad software Inc. USA). The results are presented as mean ± SEM and statistical significance determined as $p < 0.05$.

3. Results

3.1 Both FSH and hCG increase glucose uptake but only FSH upregulates glycogen synthesis

The uptake of 2-NBDG was significantly increased by FSH alone and hCG alone, but FSH was more efficient (Fig. 1A, Table 1, $p < 0.001$, $n=5$) as well as potent (Fig. 1A, Table 1, $p < 0.001$, $n=5$) than hCG (Table 1, $n=6$).

We also examined 2-NBDG incorporation into glycogen in GCs and FSH alone robustly increased the incorporation of 2-NBDG into glycogen in a concentration-dependent manner (Fig. 1B, Table 1, $p < 0.001$, $n=6$) whereas hCG alone had no significant effect (Fig. 1B, Table 1). Maximum incorporation of D-[U-^{14}C]-glucose into glycogen was observed after 4h of incubation of rat GCs with FSH (Supplemental Fig. 1).

FSH increased the uptake of glucose in GCs with EC_{50} = 0.92 ± 0.0? nM, whereas it increased the glycogen level with EC_{50} = 3.18 ± 0.07 nM. FSH concentration (1.5 nM) approximately equivalent to EC_{60} was used in subsequent experiments so as to get adequate glucose uptake for studying the inhibitory effect of hCG [32]. A concentration of FSH (3.? nM) approximately equivalent to EC_{50} was used for experiments on glycogen synthesis in GCs.

FSH increased the glycogen granules in preovulatory GCs *in vitro* in a time dependent manner up to 4h as it can be seen in the images taken under confocal microscope (Fig. 1C). But after 6h, there was no significant difference in comparison to untreated controls (Fig. 1C).

To understand the physiological importance of the observations, we examined the glycogen content in the ovaries of immature rats treated with FSH (8IU/d) for three days. As shown in Fig.1D, a robust increase in ovarian glycogen content was observed on day 1 to 3 as compared to controls ($p < 0.001$, $n=5$).

To examine whether FSH increased the activity of glycogen synthase (GS) which is a rate limiting enzyme in glycogen synthesis step, we measured the incorporation of UDP-[U-^{14}C] glucose into glycogen. Incorporation of UDP-[U-^{14}C] glucose into glycogen was stimulated by FSH with a significant increase in GS activity after 1h of treatment (Fig. 1E, $p < 0.05$, $n=3$), in a G6P-independent way. FSH also increased the protein expression of GS in preovulatory rat GCs (Supplemental Fig. 2, $p < 0.001$, $n=4$).

Increased 2-NBDG (green) co-localization with GS (red) after FSH treatment was observed by immunocytochemistry with antibodies specific to GS (Fig. 1F, lower panel; Fig. 1G, $R^2 = 0.81$, $p < 0.0001$, 10-12 cells) as compared to untreated control cells (Fig.1H, upper panel, $R^2 = 0.135$, $p = 0.425$).

To understand the effect of hCG on glycogen levels built up by FSH, GCs were treated with FSH and 2-NBDG for 4 h and then divided into 2 groups, one set of GCs were treated with hCG for another 4 h

and the other set was not treated any further and was taken as control. Glycogen content of GCs measured at the end of 4 h of incubation with FSH was taken as 100%. There was a significant decrease in the glycogen content in GCs treated with hCG for 4 h in comparison to the controls (Fig.1I, *$p < 0.05$ *vs* at time 0, $^{\#}p < 0.05$ *vs.* control, *n=3*).

To ascertain the direct role of FSH in modulation of glucose metabolism, we investigated the role of E_2 in FSH-stimulated increase in glucose uptake and glycogen synthesis in rat preovulatory GCs. FSH-stimulated glycogen was not significantly decreased in the presence of E_2 inhibitor (Fig. 1J). There was significant increase in glycogen in response to E_2 (*$p < 0.01$, *n=5* Fig. 1J) which was inhibited by anti-E_2: K-7 (*$p < 0.001$, *n=5* Fig. 1J). A significant difference between the glycogenic response of FSH and E_2 was observed (E_2: FC=1.35 ± 0.01 vs FSH: FC=2.51 ± 0.08, *$p < 0.001$, *n=5* Fig. 1J). The glycogen content was significantly decreased in GCs co-treated with FSH and E_2 in comparison to the cells treated with FSH alone (*$p < 0.001$, *n=5* Fig. 1J). There was no effect of E_2-inhibitor alone. Similar pattern of changes were observed in FSH-stimulated glucose uptake in the presence of E_2 (Supplemental Fig. 3).

3.2 FSH-stimulated glycogen synthesis in rat preovulatory GCs is dependent on IRS-2/PI3K/AKT pathway

To confirm the role of IRS-2/PI3K/Akt pathway in FSH-stimulated glycogen synthesis, firstly we checked the phosphorylation status of IRS-2. Phosphorylation of tyrosine or serine residues in IRS-2 was examined in GCs treated with FSH for 45 min. IRS-2 immunoprecipitates were analysed by Western blotting with phospho-tyrosine (p-Tyr) and phospho-serine (p-Ser)-specific monoclonal antibodies. There was a significant increase in the tyrosine phosphorylation of IRS-2 (Fig. 2A, *$p<0.05$, n=3*) and a decrease in serine phosphorylation of IRS-2 (Fig. 2B, *$p<0.05$, n=3*) in GCs treated with FSH.

Further, D-[U-^{14}C]-glucose incorporated into glycogen was measured in GCs after transfection with specific siRNA and control siRNA. A significant decrease in FSH-stimulated incorporation of D-[U-^{14}C]-glucose into glycogen was observed after knockdown of IRS-2, PI3K and Akt2 with siRNA specific to IRS-2, PI3K (P85α) and Akt2 (Fig. 2C, *$p<0.001$, n=3*), or after treatment with LY294002 and Akt inhibitor IV (Fig. 2D, *$p<0.001$, n=3*). The serine/threonine protein kinase GSK-3β inhibits GS by phosphorylation and is considered to be a major regulator of GS. We therefore investigated the effect of FSH on the phosphorylation and deactivation of GSK3β. FSH significantly increased the phosphorylation of GSK3β (5-10 fold) in GCs at Ser 9 site (Fig. 2E, F, *$p<0.001$, n=3*). GCs transfected with siRNA specific to IRS-2, PI3K (P85α) and Akt2 showed significant reduction in FSH-stimulated phosphorylation of GSK3β at Ser 9 (Fig. 2E, *$p<0.001$, n=3)* while the cells treated with scrambled siRNA sequences maintained the basal levels of phosphorylation (Fig. 2E). The cells

treated with inhibitors of PI3K (LY294002) and Akt (Akt inhibitor IV) showed marked decrease in the FSH-stimulated phosphorylation of GSK3β (Fig. 2F, *p<0.001, n=3*).

3.3 FSH activates Protein phosphatase 1 (PP1)

The activity of GS is reversibly controlled by phosphorylation/dephosphorylation mechanism, therefore, the role of phosphatases in FSH-stimulated glycogen synthesis was examined. Significant inhibition of FSH-stimulated incorporation of D-[U-^{14}C]-glucose into glycogen was observed after treatment of GCs with okadaic acid or calyculin A (Fig. 3A, *p<0.001, n=3*).

PP1 is the primary phosphatase for the activation of GS by dephosphorylation of the key phosphorylated sites of GS. Therefore, the phosphatase activity was estimated in the immune complexes of PP1 isolated from control and FSH-treated GCs. Fluorescent product (DiFMU) thus formed in the presence of PP1 was measured. After 1h of treatment, FSH had significantly increased PP1 activity in rat preovulatory GCs (Fig. 3B, *p<0.05, n=3*). A decrease in the FSH-stimulated PP1 activity was observed after treatment of GCs with PI3K inhibitor, LY294002 or Akt inhibitor IV (Fig. 3C, *p<0.05, n=3*). Both okadaic acid and calyculin A abolish PP1 activity (Fig. 3C). Further, these observations were confirmed after siRNA-mediated knockdown of IRS-2, PI3K, or AKT2, where FSH-stimulated PP1 activity was significantly inhibited in GCs (Fig. 3D, *p<0.05, n=3*).

3.4 Impairment of FSH-mediated glucose uptake and glycogen synthesis in GCs of PCOS patients with or without insulin resistance

To understand the physio-pathological significance of the regulation of glucose uptake and glycogen content in GCs by FSH, we checked both parameters in GCs of PCOS women with and without insulin resistance as well as normal ovulatory women. Patient biochemical and clinical features are given in Supplemental Table 1. FSH treatment for 1h resulted in significant increase in 2-NBDG uptake in 30 min in the GCs of normal women (Fig. 4A, *p<0.001, n=10*), but there was a significant decrease in 2-NBDG uptake in the GCs of PCOS women with and without IR (Fig. 4A, *p<0.001, n=7)*. FSH increased the glycogen content of GCs in the normal group (Fig. 4B, 4C, 4D-upper panel, *p<0.001, n=6-9*), much less in GCs of non-IR women with a significant increase only at highest concentration of FSH (4 nM) (Fig. 4B, 4C, 4D-middle panel *p<0.001, n=6-9*), but no significant increase in PCOS IR (Fig. 4B, 4C, 4D-lower panel, *n=9*). The results were comparable in both experiments where D-[U-^{14}C]-glucose (2 nM FSH, *p<0.001, n=9*) or 2-NBDG (2 nM FSH, *n=6, p<0.001*) were used as a probe. However, rate of the basal glucose uptake and glycogen synthesis were not significantly different in the GCs of normal as well as PCOS women as measured by incorporation of D-[U-^{14}C]-glucose (Fig. 4B) and 2-NBDG (Fig. 4C).

A significant number of PCOS patients with or without IR had abnormal FSH-mediated glucose uptake and glycogen synthesis (Table. 2).

3.5 Decreased glycogen content in ovaries of rat PCOS model

To validate the decrease in FSH-mediated glycogen levels in PCOS GCs, we examined the glycogen content of cystic ovaries of rats (developed by treating with antiprogestin RU486, 4mg/d, for 18 days, [17]. FSH levels were normal in PCOS rats but LH levels were 2.8±0.25 fold higher than in control rats. Glycogen content in the cystic ovaries was significantly decreased in comparison to the control ovaries of the rats in the proestrus stage (Fig. 4E, $p < 0.001$, $n=6$). Since the PCOS rats showed oestrus vaginal cell morphology [33], glycogen content was also compared with that found at oestrus stage of normal rats. The glycogen content in the ovaries at oestrous stage was significantly lower than the ovaries from the proestrous stage (Fig. 4E $p < 0.001$, $n=6$).

3.6 Inhibition of FSH-stimulated glucose uptake and glycogen synthesis by hCG

To understand the role of high LH levels in FSH-regulated glucose uptake and glycogen synthesis, GCs isolated from ovarian aspirates of normal ovulatory women after gonadotropin therapy for IVF were treated with FSH alone, hCG alone, and FSH + hCG for 3h followed by incubation with 2-NBDG (200 μM) for 30 min for glucose uptake and 3h for the estimation of glycogen content. In normal human GCs, FSH stimulated the uptake of glucose (Fig. 5A, $p < 0.001$, $n=11$) as well as the synthesis of glycogen in human GCs (Fig. 5B, $p < 0.001$, $n=10$). In comparison to the response to FSH alone, glucose uptake was significantly lower in GCs co-incubated with FSH and hCG (Fig. 5A, $p < 0.001$, $n=8$). FSH-stimulated increase in glycogen content was attenuated in the presence of hCG (Fig. 5B, $p < 0.001$, $n=9$).

Consistently, in normal rat preovulatory GCs, there was a robust inhibition of FSH-stimulated glucose uptake in the presence of hCG, when FSH was kept constant (Fig. 5C, IC_{50}= 13.05 ± 1.15 nM, $p < 0.001$, $n=6$). FSH-mediated increase in 2-NBDG incorporation in glycogen was also decreased in a dose-dependent manner in the presence of hCG (Fig. 5D, IC_{50}= 8.97 ± 1.12 nM, $p < 0.001$, $n=6$).

Further, we examined the effect of hCG *in vivo*, on the glycogen content in FSH-stimulated immature rat ovaries. Immature rats were treated with FSH alone, hCG alone and FSH + hCG for one day. Glycogen per mg ovarian weight was significantly more in FSH-treated rats (Fig. 5E, $p < 0.01$, n= 5) than in hCG-treated rats (Fig. 5E, ns, $n=5$) in comparison to untreated control animals. Rats treated with FSH + hCG had significantly lower glycogen content than FSH-treated immature rat ovaries (Fig. 5E, $p < 0.01$, n= 5).

Next, we examined the incorporation of D-[U-^{14}C]-glucose into glycogen in preovulatory rat GCs in response to insulin (10 nM) for 4h and how the presence of hCG can impact it. Insulin increased the glycogen synthesis in GCs compared to untreated cells (Fig. 5E, $p < 0.01$, n= 3) and insulin-mediated response was significantly inhibited in the presence of hCG (5-20 nM) (Fig. 5E, $p < 0.05$, $n=3$).

3.7 Downregulation of FSH-stimulated IRS-2 expression by hCG

In our earlier publication, we showed that the expression of IRS-2 was increased by FSH but not by hCG alone after 3h of treatment *in vitro* [17]. Therefore, we examined the effect of hCG on FSH-stimulated IRS-2 expression. In the presence of hCG, there was a significant decrease in FSH-stimulated IRS-2 mRNA expression in rat preovulatory GCs (Fig. 5G). However, hCG alone had no significant effect on IRS-2 mRNA expression as reported earlier [17].

3.8 Attenuation of FSH-stimulated glucose uptake by hCG in HEK293 cells expressing both LHR and FSHR

To confirm the impact of hCG on FSH-stimulated glucose uptake, we examined the uptake of 2-NBDG in HEK293 cells expressing both FLAG-LHR and HA-FSHR. When 2-NBDG uptake was examined in the presence of constant FSH (3.3 nM) and increasing hCG concentrations, the uptake of 2-NBDG was significantly inhibited at higher concentrations of hCG (Fig. 6A, Table 3, *p<0.001, n=6*). At low concentrations (0.01-0.5 nM), hCG enhanced 2-NBDG uptake by FSH (Fig. 6A, *p<0.05, n=6*). When the HEK293 cells expressing both FLAG-LHR and HA-FSHR were treated with constant hCG (3.3 nM) and increasing FSH concentrations, the inhibition of glucose uptake was at a much lower IC_{50} of FSH than IC_{50} of hCG in the last experiment (Fig. 6B, Table 3A, *p<0.001*, n=6). Basal FSH alone or hCG alone data was obtained from the same transfections as the hCG or FSH co-treatments respectively. The concentration of hCG (3.3 nM) approximately equivalent to EC_{70} was chosen so as to get adequate glucose uptake required for inhibition studies in the presence of increasing concentrations of FSH [32]. In HEK293 cells expressing both FLAG-LHR and HA-FSHR, the uptake of 2-NBDG was significantly increased by FSH alone (Fig. 6C, Table 4, *p<0.001*, n=6) and hCG alone (Fig. 6D, Table 3B, *p<0.001, n=6*).

Impact of FSH and hCG on BRET change in HEK293 cells expressing both LHR and FSHR

Heteromerization of FSHR and LHR has been indicated as a probable mechanism that may attenuate FSH actions [34]. Therefore, we studied the change in BRET signals in HEK293 cells expressing both Renilla luciferase 8 (Rluc8) tagged hFSHR and mVenus tagged hLHR. The changes in intermolecular BRET signals between sensors of hFSHR-Rluc8 and hLHR-Venus were monitored upon stimulation of these cells with increasing concentrations (10 pM to 100 nM) of FSH or hCG in the presence of a constant concentration (3.3 nM) of hCG or FSH respectively. BRET signal change w.r.t untreated cells was measured. A robust increase in BRET signals was elicited in the presence of increasing concentrations of FSH in the presence of a fixed concentration of hCG (Fig. 6E, EC_{50} =1.12 ± 0.02 nM, *p<0.0001, n=5*). Although, the BRET signals increased significantly in response to varying concentrations of hCG in the presence of constant FSH (Fig. 6F, *p<0.021, n=5*), the concentration dependence of changes in BRET signals was not as robust as seen with varying concentration of FSH and constant hCG. The BRET signals did not increase in the presence of FSH alone (Fig. 6G) or hCG

alone (Fig. 6H). Taken together, real-time kinetic analysis of BRET signals in HEK293 cells expressing hFSHR-Rluc8 and hLHR-Venus and stimulated with both hCG and FSH showed a significant increase in the proximity of FSHR and LHR receptors leading to heteromerization. In other words, the difference in the BRET signals elicited by different ratios of FSH:hCG suggests the existence of hormone-specific regulation of FSHR-LHR heteromerization.

4. Discussion

This study demonstrates for the first time the upregulation of glycogen synthesis in preovulatory GCs by FSH through IRS-2/PI3K/Akt2 pathway. Interestingly, hCG had no robust effect on glycogen synthesis, rather in preovulatory rat GCs, it was more glycolytic than FSH. These findings confirm that FSH is the key driver for glycogen synthesis through increase in glycogen synthase activity in preovulatory GCs. It is noteworthy that FSH not only increases the activity of glycogen synthase but also its protein expression in preovulatory GCs. Our earlier and the present study provide evidence that FSH stimulates the expression as well as the activity of IRS-2, which is involved in signaling cascades of insulin, IGF-1, interleukin, IFN, growth hormone and integrins, and may be an important component in the complex cross-talk between their receptors [22-24, 35]. This is corroborated by the fact that the absence of InsR in GCs does not adversely affect the fertility of mice in terms of pups per litter or the number of oocytes ovulated [25]. The novel mechanisms of FSH action are now becoming clear and add to our understanding about the complex processes involved in metabolic homeostasis during folliculogenesis. Apparently, signaling through a limited type of effectors may not be sufficient for FSHR and it may cross-regulate the signaling pathways of other GPCRs or RTKs, thereby leading to diverse physiological responses during follicular maturation [17, 36-38].

In preovulatory GCs, FSH-mediated glycogen stores may either have a basic role of energy reserve (as glucose or lactate) in the growing follicles, or it may be important for other metabolic pathways required for the complex processes of folliculogenesis, oocyte maturation and ovulation. Glycogen may be important for generation of nucleotides required for DNA repair, proliferation of GCs and neutralizing the oxidative stress in the growing follicles. Glycogen may help in cell survival in the hypoxic environment of the preovulatory follicles [39]. In addition, glycogen may work like a metabolic sensor in preovulatory follicles due to its tight metabolic coupling with that of lipids [40-41].

We had earlier demonstrated that upregulation of IRS-2 expression by FSH was crucial for activation of PI3K/Akt pathway and glucose uptake in preovulatory rat GCs [17]. Here, we demonstrate an insulin-independent increase in tyrosine phosphorylation, decrease in Ser/Thr phosphorylation and activation of IRS-2 by FSH, however further studies are needed to understand the underlying mechanisms. IRS-2 is activated by phosphorylation of its tyrosine residues, thereby initiating the signaling cascades [42]. It is also regulated by phosphorylation status of specific serine residues leading to either decrease or increase in its activity [43]. Additionally, FSH-stimulated PKA may increase IRS-2 protein stability by phosphorylation of certain Ser/Thr residues [43]. We also need to find the specific tyrosines of IRS-2 that are phosphorylated and whether these tyrosine residues are different from the ones phosphorylated in response to insulin [42, 44].

The physiological importance of the upregulation of glycogen synthesis by FSH was substantiated by our findings, where there were defects in FSH-stimulated glucose uptake and glycogen levels in GCs of both insulin resistant as well as non-insulin resistant PCOS patients [17]. Interestingly, insulin-stimulated glycogen synthesis through its receptor was found to be normal in PCOS patients but at higher concentrations of insulin it could not elicit an appropriate response [4, 22, 45]. The tyrosine kinase domain of InsR gene is normal in women with hyperinsulinaemia and PCOS [46]. An increase in mitogenic activity by IGF-1 has been reported in PCOS [22]. A decrease in FSH-stimulated IRS-2 levels would limit its availability to insulin receptors. This is corroborated by our earlier findings which demonstrated a defect in FSH-stimulated expression of IRS-2 in PCOS GCs [17]. In view of normal or hyper-steroidogenic responses of insulin as well as FSH in PCOS women, these novel findings indicate that the impairment of metabolic pathways in PCOS GCs are due to defective FSH signaling caused by higher than normal levels of LH. The findings here establish the deleterious effects of high LHR activity on FSH-mediated glucose uptake and glycogen synthesis in PCOS GCs. This study provides an important model system for understanding the mechanism of selective FSH resistance in PCOS patients which may increase their susceptibility to develop insulin resistance later in life.

One of the biochemical consequences of high LH is hyperandrogenism, predominantly of ovarian origin, in PCOS patients. Several lines of evidence have linked elevated androgen levels with insulin resistance, but most studies have been inconclusive while conferring a direct role upon androgens [27, 47-50]. This is further supported by the fact that the androgen receptor (AR) antagonists are not able to reverse high testosterone-linked insulin resistance [47-48, 51]. Suppression of hypothalamic-pituitary axis with GnRH analogues did show improvement in insulin sensitivity in PCOS women with hyperandrogenism but not in all studies [52-55]. Mechanisms by which androgens may adversely affect insulin sensitivity in women with PCOS may include indirect androgenic actions or non-androgenic mechanisms including defective lipolysis in adipocytes, oxidative stress, beta cells dysfunction and increase in the secretion of insulin [48, 56-57].

Notwithstanding, several other studies have supported the association of high testosterone with insulin sensitivity in males, but later it was elucidated to be through its conversion to E_2 and its action via ER [27, 56-61]. Both physiological and genetic evidences favored the role of E_2 in insulin sensitivity, but supra-physiological levels of E_2 or T were found to increase insulin-stimulated inhibitory phosphorylation of IRS-1^{Ser636} but these studies could not be confirmed by other groups [48-49, 62]. A robust evidence is still lacking on the direct effect of E_2 and T on glucose metabolism especially in ovary or in GCs and would be an interesting aspect for further study. In a study by Gibbs and colleagues [63], healthy men treated with aromatase inhibitor showed reduction in insulin sensitivity. Intriguingly, in addition to low estrogen levels in their plasma, they had significantly high levels of LH.

To understand the complexity of FSH-mediated glucose metabolism in preovulatory GCs, we checked the effect of E_2 on FSH-stimulated glycogen synthesis. E_2 alone increased the glycogen synthesis but it was not as robust as observed with FSH alone. It was intriguing to find that the same concentration of E_2 caused a slight, though significant, decrease in the FSH-stimulated synthesis of glycogen. Similar effect of E_2 was seen on glucose uptake in GCs. Overall, our findings here show a major role of FSH in glucose uptake and glycogen synthesis in preovulatory GCs, which is impeded by abnormally high LHR activity.

Several studies have elaborated on the role of FSH, LH and insulin in the maintenance of energy substrates in the oocytes of preantral/antral stages or cumulus-oocyte complexes, however our understanding of the regulation of glucose metabolism in the preovulatory stage is limited to the production of lactate and pyruvate [12, 64-66]. The significance of glycolysis and lactate production in gonadotropin-induced follicle maturation is still controversial [67]. Also, the role of insulin during folliculogenesis is not clear and future studies will be required to understand the selective modulation of insulin signaling by FSH and LH. Previously, Ma *et al.*, 2015 [68] reported that high LH attenuates insulin sensitivity in adipocytes, and we found it to be true in GCs as well.

There has been a controversy on the optimal doses of LH to be included in the ovarian stimulation protocol of IVF for PCOS patients, an aspect that has confounded the investigators over the last two decades [69-70]. Exposure to high LH during early follicular phase has been shown to be associated with poor maturation of oocytes and reduced fertilization rate in PCOS women [5, 69]. To address the issues arising due to high LH, we studied the concentration-dependent effects of hCG on the FSH responses such as glucose uptake and glycogen synthesis. Interestingly, a synergistic effect of very low concentrations of hCG on FSH-stimulated glucose uptake was observed. However, at higher concentrations, it had adverse effects on FSH-mediated glucose uptake and glycogen synthesis in human and rat GCs. A selective heterologous desensitization of FSHR is observed in the presence of high hCG such that stimulation of IRS-2 expression by FSH was inhibited. Our findings support the relative importance of FSH and hCG in the modulation of glucose uptake and glycogen storage in GCs over the other intra-ovarian growth factors like insulin, IGF-1, EGF, and TGF-β1 [17, 71].

Both LH and hCG bind and signal through the same receptor designated as LHR or LHCGR. Casarini and colleagues [72-74] have demonstrated that hCG is 5-fold more potent than LH in binding LHR and activating cAMP/PKA pathway in heterologous cell lines expressing LHR and gonadal cells. However, there is no significant difference in the maximal testosterone response produced by LH and hCG [73]. But, LH and hCG differentially modulate progesterone and proliferative responses in granulosa-lutein cells *in vitro* in the presence of FSH [75-76]. Studies are required to confirm whether FSH has different mechanisms of cross-talk with hCG and LH to modulate glucose uptake and glycogen synthesis, which may be a limitation of the present study.

In HEK293 cells co-expressing FSHR and LHR, we observed an increase in the proximity of FSHR and LHR and a concomitant decrease in FSH-stimulated glucose uptake, when exposed to both hCG and FSH. A larger picture is emerging here with a positive cross-talk of FSHR with InsR signaling pathways through IRS-2 and a negative one with higher concentration of hCG or LH as in PCOS patients. The glycoprotein receptors (FSHR, LHR, TSHR) have been found to make dimers or trimers [32]. While LHR and FSHR form heteromers, heteromerization is known to attenuate the hormone-dependent signaling by reducing the cAMP production [34] or prolonging the Ca^{2+} response of the LHR [77]. Interestingly, this is the first report of a functional correlation of the FSHR-LHR heteromerization with reduction in FSH-stimulated glucose uptake. However, further studies are required to elucidate the mechanism (s) of attenuation of FSH-stimulated glucose uptake caused by high concentrations of LH through FSHR-LHR heteromerization.

Most of the earlier studies have demonstrated the regulation of GPCRs by RTKs [34, 78]. The transactivation of heterologous receptors by a GPCR may have different consequences [79-80]. Angiotensin II increased the phosphorylation of IRS-1 and IRS-2 through its GPCR, but attenuated the insulin-stimulated PI3K activity [80]. In contrast, insulin induced desensitization of β_2Adrenergic receptor (β_2AR) was in an IRS-1/IRS-2 dependent manner [78]. Our earlier findings and the ones reported here present compelling evidence for an insulin-independent regulation of glucose metabolism by FSH which happens through increase in expression as well as tyrosine phosphorylation of IRS-2 leading to the upregulation of glucose uptake and glycogen synthesis in preovulatory GCs. Additionally, it is pertinent to accept the transactivation of post-receptor signaling mechanisms of insulin by FSH and its impact on insulin responses.

In summary, our findings demonstrate a crucial role of FSH in glucose metabolism in preovulatory follicles. FSH is more efficient as well as potent in stimulating glucose uptake in GCs than hCG. Storage of glucose as glycogen is regulated by FSH through IRS-2/PI3K/Akt2 pathway in preovulatory GCs. Whereas, hCG not only increases glycogen depletion but also inhibits the FSH-stimulated IRS-2 expression, glucose uptake and glycogen synthesis (Fig. 7). FSH-stimulated glucose uptake and storage are impaired in women with PCOS, indicating a selective defect in FSHR activation. Interference of the FSH-stimulated glucose uptake and storage by high LH would lead to intra-ovarian glycogen deficit in PCOS patients causing follicle growth arrest and anovulation in the PCOS patients (Fig. 7). The low levels of IRS-2 in GCs may contribute to the intra-ovarian insulin resistance in PCOS patients. Together these data identify a novel mechanism of cross-talk between the FSH, LH and insulin signaling pathways to maintain metabolic homeostasis in GCs.

In conclusion, this is the first report on the FSH- and LH-mediated integrated regulation of glucose and glycogen levels in preovulatory GCs and any defect in this cross-talk may have a greater impact in the pathogenesis of PCOS (Fig. 7). These data suggest a therapeutic potential of LH antagonists in the management of metabolic syndrome in PCOS patients.

Disclosure of competing interest:

The authors have no conflicts of interest and declare no competing financial interests.

Acknowledgments

This study was supported by research grant no. BT/PR10379/MED/97/215/2013 of Department of Biotechnology (DBT) and grant no. RC/2015/9677/D-1813 of University of Delhi, Delhi, India to RS. I greatly acknowledge Dr. Aylin C. Hanyaloglu (Imperial College London, London, UK) who provided HEK293 cells, Flag-LHR and HA-FSHR plasmids. We are thankful to Dr. Satish K. Gupta, NII for his help in the import of HEK293 cells in NII and Dr. Smita Bhatia for critical review of the manuscript. We thank all women who participated in this study.

Consent for publication

All authors have approved the manuscript for submission.

Funding source

This study was supported by research grant of RS, Grant no. BT/PR10379/MED/97/215/2013 from Department of Biotechnology (DBT), India and grant no. RC/2015/9677/D-1813 from University of Delhi, Delhi, India.

Authors' role

NC and AG have contributed equally to the manuscript. Experiments other than BRET change were performed in the laboratory of RS by AG, NC, SK, RL, and AN. NM and MGD provided human samples and patient data. RS, KMD and TGS analysed the results. RS and FP did the BRET experiments. PC and ER coordinated the BRET investigations. RS designed the study, wrote the manuscript and contributed to the experiments. Coordination of the work outlined in the manuscript and supervision of the accuracy of the information was also done by RS. All authors critically read and approved the manuscript.

References

1. Apridonidze T, Essah PA, Iuorno MJ, Nestler JE. Prevalence and characteristics of the metabolic syndrome in women with polycystic ovary syndrome. Journal of Clinical Endocrinology and Metabolism 2005;90(4):1929–1935.
2. Azziz R, Carmina E, Dewailly D, et al. Task Force on the Phenotype of the Polycystic Ovary Syndrome of The Androgen Excess and PCOS Society. The Androgen Excess and PCOS Society criteria for the polycystic ovary syndrome: the complete task force report. Fertil Steril 2009;91(2):456-88.
3. Kaur S, Archer KJ, Gouri Devi M, et al. Differential gene expression in granulosa cells from polycystic ovary syndrome patients with and without insulin resistance: Identification of susceptibility gene sets through network analysis. J Clin Endocrinol Metab 2012;97:E2016-E2021.
4. Rice S, Christoforidis N, Gadd C, et al. Impaired insulin-dependent glucose metabolism in granulosa-lutein cells from anovulatory women with polycystic ovaries. Hum Reprod 2005;20:373-381.
5. Willis DS, Watson H, Mason HD, et al. Premature response to luteinizing hormone of granulosa cells from anovulatory women with polycystic ovary syndrome: relevance to mechanism of anovulation. J Clin Endocrinol Metab 1998;83:3984-3991.
6. Yen SSC, Vela P, Rankin J. Inappropriate secretion of follicle-stimulating hormone and luteinizing hormone in polycystic ovarian disease. J Clin Endocrinol Metab1970;30:435–442.
7. Kazer RR, Kessel B, Yen SSC. Circulating luteinizing hormone pulse frequency in women with polycystic ovary syndrome. J Clin Endocrinol Metab1987;65:233–236.
8. Risma KA, Clay CM, Nett TM, et al. Targeted overexpression of luteinizing hormone in transgenic mice leads to infertility, polycystic ovaries, and ovarian tumors. Proc Natl Acad Sci USA 1995;92:1322-1326.
9. Matzuk MM, DeMayo FJ, Hadsell LA, Kumar TR. Overexpression of human chorionic gonadotropin causes multiple reproductive defects in transgenic mice. Biol Reprod 2003;69:338-346.
10. Orisaka M, Hattori K, Fukuda S, et al. Dysregulation of ovarian follicular development in female rat: LH decreases FSH sensitivity during preantral-early antral transition. Endocrinology 2013;154:2870-2880.
11. Guedikian AA, Lee AY, Grogan TR, et al. Reproductive and metabolic determinants of granulosa cell dysfunction in normal-weight women with polycystic ovary syndrome. Fertil Steril 2018;109(3):508-515.

12. Zuelke KA, Brackett BG. Effects of luteinizing hormone on glucose metabolism in cumulus-enclosed bovine oocytes matured in vitro. Endocrinology 1992;131:2690-2696.

13. Harlow CR, Winston RM, Margara RA, Hillier SG. Gonadotrophic control of human granulosa cell glycolysis. Hum Reprod 1987;2(8):649-653.

14. Cran DG, Hay MF, Moor RM. The fine structure of the cumulus oophorus during follicular development in sheep. Cell Tissue Res 1979;202(3):439-451.

15. Singh UP, Krishna A. Glycogen accumulation in the ovarian follicle of Indian vespertilionid bat, Scotophilus heathi during the period of delayed ovulation. Zoolog Sci 1996;13(6):893-897.

16. Otani T, Maruo T, Yukimura N, Mochizuki M. Effect of insulin on porcine granulosa cells: implications of a possible receptor mediated action. Acta Endocrinol (Copenh)1985;108:104-110.

17. Anjali G, Kaur S, Lakra R, et al. FSH stimulates IRS-2 expression in human granulosa cells through cAMP/SP1, an inoperative FSH action in PCOS patients. Cellular Signal 2015;27:2452-2466.

18. Ulloa-Aguirre A, Reiter E, Crépieux P. FSH Receptor Signaling: Complexity of interactions and Signal Diversity. Endocrinology 2018;159(8):3020-3035.

19. Ascoli M, Fanelli F, Segaloff DL. The lutropin/choriogonadotropin receptor, a 2002 perspective. Endocr Rev 2002;23:141-174.

20. Dierich A, Sairam MR, Monaco L, et al. Impairing follicle-stimulating hormone (FSH) signaling in vivo: targeted disruption of the FSH receptor leads to aberrant gametogenesis and hormonal imbalance. Proc Natl Acad Sci USA 1998;95:13612-13617.

21. Catteau-Jonard S, Jamin SP, Leclerc A, et al. Anti-Mullerian hormone, its receptor, FSH receptor, and androgen receptor genes are overexpressed by granulosa cells from stimulated follicles in women with polycystic ovary syndrome. J Clin Endocrinol Metab 2008;93(11):4456-4461.

22. Wu XK, Zhou SY, Liu JX, et al. Selective ovary resistance to insulin signaling in women with polycystic ovary syndrome. Fertil Steril 2003;80:954-965.

23. Wu X, Sallinen K, Anttila L, et al. Expression of insulin-receptor substrate-1 and -2 in ovaries from women with insulin resistance and from controls. Fertil Steril 2000;74:564-572.

24. Burks DJ, Font de Mora J, Schubert M, et al. IRS-2 pathways integrate female reproduction and energy homeostasis. Nature 2000;407:377-382.

25. Baumgarten SC, Armouti M, Ko C, Stocco C. IGF1R Expression in Ovarian Granulosa Cells Is Essential for Steroidogenesis, Follicle Survival, and Fertility in Female Mice. Endocrinology. 2017;158(7):2309-2318.

26. Rotterdam ESHRE/ASRM-Sponsored PCOS Consensus Workshop Group. Revised 2003 consensus on diagnostic criteria and long-term health risks related to polycystic ovary syndrome (PCOS). Human Reproduction. 2004;19(1):41-74.

27. Barros RPD, Morani A, Moriscot A, Machado UF. Insulin resistance of pregnancy involves estrogen-induced repression of muscle GLUT4. Mol Cell Endocrinol 2008;295(1-2):24-31.

28. Singh R. Antifertility potential of 2-[piperdinoethoxy phenyl]-3-[4-methoxy phenyl]-2H benzo pyran: a potent antioestrogenic compound in rats. J Reproduction & Fertility 1996;106:49-53.

29. Louzao MC, Espiña B, Vieytes MR, et al. "Fluorescent glycogen" formation with sensibility for *in vivo* and *in vitro* detection. Glycoconj J 2008;25:503-510.

30. Rasouli M, Ostovar-Ravari A, Shokri-Afra H. Characterization and improvement of phenol-sulfuric acid microassay for glucose-based glycogen. Eur Rev Med Pharmacol Sci 2014;18:2020-2024.

31. Gee KR, Sun WC, Bhalgat MK, et al. Fluorogenic substrates based on fluorinated umbelliferones for continuous assays of phosphatases and beta-galactosidases. Anal Biochem1999;273(1):41-48.

32. Jiang X, Fischer D, Chen X, et al. Evidence for Follicle-stimulating Hormone Receptor as a Functional Trimer. J Biol Chem. 2014;289(20):14273-14282.

33. Sánchez-Criado JE, Sánchez A, Ruiz A, Gayán F. Endocrine and morphological features of cystic ovarian condition in antiprogesterone RU486-treated rats. Acta Endocrinol (Copenh) 1993 Sep;129(3):237-245.

34. Feng X, Zhang M, Guan R, Segaloff DL. Heterodimerization between the lutropin and follitropin receptors is associated with an attenuation of hormone-dependent signaling. Endocrinology 2013;154:3925-3930.

35. Argetsinger LS, Norstedt G, Billestrup N, White MF, Carter-Su C. Growth hormone, interferon-gamma, and leukemia inhibitory factor utilize insulin receptor substrate-2 in intracellular signaling. J Biol Chem 1996;271(46):29415-29421.

36. Law NC, Donaubauer EM, Zeleznik AJ, Hunzicker-Dunn M. How protein kinase A activates canonical tyrosine kinase signaling pathways to promote granulosa cell differentiation. Endocrinology 2017;158(7):2043-2051.

37. Hur EM, Kim KT. G protein-coupled receptor signalling and cross-talk: achieving rapidity and specificity. Cell Signal 2002;14(5):397-405.

38. Fu Q, Shi Q, West TM, Xiang YK. Cross-Talk Between Insulin Signaling and G Protein-Coupled Receptors. J Cardiovasc Pharmacol 2017;70(2):74-86.

39. Iida Y, Aoki K, Asakura T, et al. Hypoxia promotes glycogen synthesis and accumulation in human ovarian clear cell carcinoma. Int J Oncol 2012;40:2122-2130.

40. Meléndez R, Meléndez-Hevia E, Cascante M. How did glycogen structure evolve to satisfy the requirement for rapid mobilization of glucose? A problem of physical constraints in structure building. J Mol Evol 1997;45(4):446-455.

41. Markan KR, Jurczak MJ, Brady MJ. Stranger in a strange land: roles of glycogen turnover in adipose tissue metabolism. Mol Cell Endocrinol 2010;318(1-2):54-60.

42. Rojas FA, Hirata AE, Saad MJ. Regulation of insulin receptor substrate-2 tyrosine phosphorylation in animal models of insulin resistance. Endocrine 2003;21:115-122.

43. Neukamm SS, Ott J, Dammeier S, et al. Phosphorylation of serine 1137/1138 of mouse insulin receptor substrate (IRS) 2 regulates cAMP-dependent binding to 14-3-3 proteins and IRS2 protein degradation. J Biol Chem 2013;288:16403-16515.

44. Musnier A, Heitzler D, Boulo T, et al. Developmental regulation of p70 S6 kinase by a G protein-coupled receptor dynamically modelized in primary cells. Cell Mol Life Sci 2009;66:3487-3503.

45. Willis D, Franks S. Insulin action in human granulosa cells from normal and polycystic ovaries is mediated by the insulin receptor and not the type I insulin-like growth factor receptor. J Clin Endocrinol Metab 1995;80(12):3788-3790.

46. Conway GS, Avey C, Rumsby G. The tyrosine kinase domain of the insulin receptor gene is normal in women with hyperinsulinaemia and polycystic ovary syndrome. Hum Reprod 1994;9:1681-1683.

47. Corbould A. Effects of androgens on insulin action in women: is androgen excess a component of female metabolic syndrome? Diabetes Metab Res Rev 2008;24:520-532.

48. Diamanti-Kandarakis E, Mitrakou A, Hennes MMI, et al. Insulin sensitivity and antiandrogenic therapy in women with polycystic ovary syndrome. Metabolism 1995;44:525–561.

49. Garrido P, Salehzadeh F, Duque-Guimaraes DE, Al-Khalili L. Negative regulation of glucose metabolism in human myotubes by supraphysiological doses of 17β-estradiol or testosterone. Metabolism 2014;63(9):1178-1187.

50. Polderman KH, Gooren LJ, Asscheman H, Bakker A, Heine RJ. Induction of insulin resistance by androgens and estrogens. J Clin Endocrinol Metab 1994;79:265-271.

51. Moghetti P, Tosi F, Castello R, et al. The insulin resistance in women with hyperandrogenism is partially reversed by antiandrogen treatment: evidence that androgens impair insulin action in women. J Clin Endocrinol Metab 1996; 81: 952–960.

52. Krotkiewski M, Landin K, Dahlgren E, Janson PO, Holm G. Effect of two modes of antiandrogen treatment on insulin sensitivity and serum leptin in women with PCOS. Gynecol Obstet Invest 2003;55:88-95.

53. Dahlgren E, Landin K, Krotkiewski M, Holm G, Janson PO. Effects of two antiandrogen treatments on hirsutism and insulin sensitivity in women with polycystic ovary syndrome. Hum Reprod 1998;13:2706-2711.

54. Diamanti-Kandarakis E, Mitrakou A, Raptis S, Tolis G, Duleba AJ. The effect of a pure antiandrogen receptor blocker, flutamide, on the lipid profile in the polycystic ovary syndrome, J Clin Endocrinol Metab 1998;83:2699-2705.

55. Dunaif A, Green G, Futterweit W, Dobrjansky A. Suppression of hyperandrogenism does not improve peripheral or hepatic insulin resistance in the polycystic ovary syndrome. J Clin Endocrinol Metab 1990;70:699-704.

56. Moverare-Skrtic S, Venken K, Andersson N, et al. Dihydrotestosterone treatment results in obesity and altered lipid metabolism in orchidectomized mice. Obesity (Silver Spring) 2006;14:662-672.

57. Navarro G, Allard C, Xu W, Mauvais-Jarvis F. The role of androgens in metabolism, obesity, and diabetes in males and females. Obesity (Silver Spring). 2015;23(4):713-719.

58. Mauvais-Jarvis F, Clegg DJ, Hevener AL. The role of estrogens in control of energy balance and glucose homeostasis. Endocr Rev 2013;34:309-338.

59. Russell N, Grossmann M. Mechanisms in Endocrinology: Estradiol as a male hormone. Eur J Endocrinol 2019;181(1):R23-R43.

60. Pitteloud N, Mootha VK, Dwyer AA, et al. Relationship between testosterone levels, insulin sensitivity, and mitochondrial function in men. Diabetes Care 2005;28:1636-1642.

61. Riant E, Waget A, Cogo H, et al. Estrogens protect against high-fat diet-induced insulin resistance and glucose intolerance in mice. Endocrinology. 2009 May;150(5):2109-2117.

62. Kempegowda P, Melson E, Manolopoulos KN, Arlt W, O'Reilly MW. Implicating androgen excess in propagating metabolic disease in polycystic ovary syndrome. Ther Adv Endocrinol Metab 2020;11:2042018820934319.

63. Gibb FW, Homer NZM, Faqehi AMM, et al. Aromatase inhibition reduces insulin sensitivity in healthy men. J Clin Endocrinol Metab 2016;101:2040–2046.

64. Roberts R, Stark J, Iatropoulou A, et al. Energy substrate metabolism of mouse cumulus-oocyte complexes: response to follicle-stimulating hormone is mediated by the phosphatidylinositol 3-kinase pathway and is associated with oocyte maturation. Biol Reprod 2004;71:199-209.

65. Hillensjö T, Bauminger S, Ahrén K. Effect of luteinizing hormone on the pattern of steroid production by preovulatory follicles of pregnant mare's serum gonadotropin-injected immature rats. Endocrinology 1976;99(4):996-1002.

66. Sutton-McDowall, ML, Gilchrist, RB and Thompson, JG. The pivotal role of glucose metabolism in determining oocyte developmental competence. Reproduction 2010;139:685–695.

67. Tsafriri A, Lieberman ME, Ahrén K, Lindner HR. Dissociation between LH-induced aerobic glycolysis and oocyte maturation in cultured Graafian follicles of the rat. Acta Endocrinol (Copenh). 1976;81(2):362-366.

68. Ma Q, Fan J, Wang J, et al. High levels of chorionic gonadotrophin attenuate insulin sensitivity and promote inflammation in adipocytes. J Mol Endocrinol 2015;54:161-170.

69. Kolibianakis EM, Albano C, Kahn J, et al. Exposure to high levels of luteinizing hormone and estradiol in the early follicular phase of gonadotropin-releasing hormone antagonist cycles is associated with a reduced chance of pregnancy. Fertil Steril 2003, 79(4):873-880.

70. Westergaard LG, Laursen SB, Andersen CY. Increased risk of early pregnancy loss by profound suppression of luteinizing hormone during ovarian stimulation in normogonadotrophic women undergoing assisted reproduction. Hum Reprod 2000;15(5):1003-1008.

71. Roy SK, Terada DM, Activities of glucose metabolic enzymes in human preantral follicles: in vitro modulation by follicle-stimulating hormone, luteinizing hormone, epidermal growth factor, insulin-like growth factor I, and transforming growth factor beta1. Biol Reprod 1999;60:763-768.

72. Casarini L, Lispi M, Longobardi S, et al. LH and hCG action on the same receptor results in quantitatively and qualitatively different intracellular signalling. PLoS One 2012;7(10):e46682.

73. Riccetti L, Yvinec R, Klett D, et al. Human Luteinizing Hormone and Chorionic Gonadotropin Display Biased Agonism at the LH and LH/CG Receptors. Sci Rep. 2017;7(1):940.

74. Casarini L, Riccetti L, De Pascali F, et al. Estrogen Modulates Specific Life and Death Signals Induced by LH and hCG in Human Primary Granulosa Cells In Vitro. Int J Mol Sci. 2017;18(5):926.

75. Gupta C, Chapekar T, Chhabra Y, et al. Differential response to sustained stimulation by hCG & LH on goat ovarian granulosa cells. Indian J. Med. Res. 2012;135:331-340.

76. Casarini, L. Riccetti, L. de Pascali, F, et al. Follicle-stimulating hormone potentiates the steroidogenic activity of chorionic gonadotropin and the anti-apoptotic activity of luteinizing hormone in human granulosa-lutein cells in vitro. Mol. Cell. Endocrinol 2016;422:103-114.

77. Jonas KC, Chen S, Virta M, et al. Temporal reprogramming of calcium signalling via crosstalk of gonadotrophin receptors that associate as functionally asymmetric heteromers. Sci Rep. 2018;8(1):2239(1-11).

78. Karoor V, Malbon CC. Insulin-like growth factor receptor-1 stimulates phosphorylation of the beta2-adrenergic receptor in vivo on sites distinct from those phosphorylated in response to insulin. J Biol Chem 1996;271(46):29347-29352.

79. Jeoung M, Lee C, Ji I, Ji TH. Trans-activation, cis-activation and signal selection of gonadotropin receptors. Mol Cell Endocrinol 2007;260-262:137-143.

80. Velloso LA, Folli F, Sun XJ, et al. Cross-talk between the insulin and angiotensin signaling systems. Proc Natl Acad Sci USA 1996;93(22):12490-12495.

Figure Legends

Fig. 1. Glucose uptake is increased by both FSH and hCG whereas glycogen synthesis is upregulated only by FSH. (A) Glucose uptake in rat preovulatory GCs treated with FSH alone or hCG alone for 1h before the addition of 2-NBDG for 30 min. (B) Incorporation of 2-NBDG into glycogen for 4 h in the presence of FSH. (C) 2-NBDG-labelled glycogen granules in rat GCs after varying time periods of FSH treatment (1-8 h). 2-NBDG incorporated into glycogen was observed under confocal microscope and was quantified using Image J software. Scale bar, 20 µm, lower 2 panels, and 10 µm, upper panel. (D) Glycogen content in immature rat ovaries increased after FSH treatment on day 1-3. (E) Activation of glycogen synthase (GS) after treatment with FSH in a G6P-independent manner. GS activity was quantified as nmoles of UDP-glucose incorporated/mg protein/h. (F) FSH increased the co-localization of glycogen granules and GS (Upper panel) in comparison to control (Lower panel). 2-NBDG incorporated into glycogen was observed under confocal microscope and was quantified using Image J software. Scale bar, 20 µm. (G) Regression analysis of FSH-treated GCs as in F (Upper panel). (H) Regression analysis of untreated GCs as in F (Lower panel). (I) Increased depletion of glycogen in GCs in the presence of hCG (Red line) than in control cells (blue line). (J) Effect of E_2 on FSH-stimulated increase in glycogen. Rat preovulatory GCs were treated with FSH (3.3 nM), E_2 (50 nM) and E_2 inhibitor (AntiE$_2$ K-7, 4µg/ml) or in combination for 1h before addition of 2-NBDG for 3h. All data are expressed as Mean ± SEM (n= 4-6), *p< 0.001 *vs.* untreated cells, $^{\#}p$< 0.001*vs.* FSH treated.

Fig. 2. FSH upregulates glycogen synthesis in rat preovulatory GCs through IRS-2/PI3K/Akt2 pathway. (A) FSH-mediated increase in p-Tyr staining in IRS-2 immune complexes in comparison to control GCs. (B) Decrease in p-Ser staining in IRS-2 immune complexes from FSH treated GCs in comparison to control GCs. Western blotting was performed using IRS-2, p-Tyr and p-Ser-specific antibodies on immune complexes precipitated with IRS-2 specific antibody. Densitometry analysis of p-Tyr and p-Ser is shown in histograms after normalization with corresponding IRS-2 protein densities. (C) FSH-stimulated incorporation of D-[U-^{14}C]-glucose into glycogen after siRNA-mediated knockdown of PI3K, Akt2 and IRS-2. Scrambled siRNA transfected GCs were taken as control. (D) Inhibition of FSH-mediated increase in glycogen in the presence of 10 µM LY294002 (PI3K inhibitor) and 7µM Akt inhibitor IV. (E) Inhibition of increase in p-GSK3β by FSH after siRNA-mediated knockdown of PI3K, Akt2 and IRS-2. Scrambled siRNA transfected GCs were used as control. (F) Inhibition of FSH-mediated increase in p-GSK3β on preincubation with LY294002 and Akt inhibitor IV. The data are presented as mean ± SEM of 3 independent experiments (n = 3), *p< *0.001 vs.* untreated cells, $^{\#}p$< 0.001*vs.* FSH treated.

Fig. 3. Activation of protein phosphatase 1 (PP1) in preovulatory rat GCs by FSH. (A) FSH-mediated glycogen synthesis in the presence of phosphatase inhibitors, okadaic acid (10 nM) and calyculin A (0.5 nM) when treated for 30 min prior to treatment with FSH for 4 h. (B) PP1 activity in FSH-treated rat GCs (filled circle) and untreated control GCs (empty circle) for different time periods. Immune complexes of PP1 isolated from FSH-treated and control GCs were processed for the estimation of PP1 activity as described in methods section. (C) GCs were pre-treated with PI3K inhibitors LY294002 (50 μM), Akt inhibitor IV (7 μM), okadaic acid, and calyculin A for 30 min prior to treatment of FSH for 1 h and PP1 activity was measured in its immune complexes. (D) PP1 activity in rat GCs transfected with PI3K, AKT and IRS-2 siRNA prior to FSH treatment. GCs transfected with scrambled siRNA were used as control. Data are presented as mean ± SEM from three independent experiments (n = 3). *$p < 0.05$ *vs.* untreated, $^{\#}p < 0.05$ *vs.* FSH treated.

Fig. 4. FSH-stimulated glucose metabolism in Normal, PCOS non-IR and PCOS-IR human GCs and in ovaries of rat model of PCOS. (A) Human GCs from Normal, PCOS-IR and PCOS non-IR women were incubated with FSH (3.3 nM) for 1h, *in vitro* and 2-NBDG uptake was monitored 30 mins after the incubation (n=7-10). (B) D-[U-^{14}C]-glucose incorporation into glycogen in human GCs (n=6) was measured after 4h of treatment with different concentrations of FSH. (C) 2-NBDG incorporation into glycogen in human GCs after treatment with FSH for 4h (n=6). (D) Confocal images of 2-NBDG incorporation into glycogen (green) in human GCs on culture slides. DAPI (blue) was used for counterstaining of nuclei. Images of cells were analysed and Image J software was used for the quantification of fluorescence intensities. Scale bar, 20 μm. (E) Glycogen content in cystic ovaries of RU486-treated rat PCOS model. Values presented are the mean ± SEM (n = 5-10), *$p < 0.001$ *vs.* untreated control.

Fig. 5. Effect of hCG on FSH-stimulated glucose uptake and glycogen synthesis. (A) 2-NBDG uptake in human GCs on treatment with FSH alone and hCG alone. The presence of hCG inhibited the FSH-stimulated 2-NBDG uptake (B) Incorporation of 2-NBDG into glycogen in human GCs, it is inhibited in the presence of FSH+ hCG. (C) Uptake of 2-NBDG was inhibited in normal rat GCs treated with FSH (3.3 nM) and variable hCG (Red) for 30 min. (D) Glycogen synthesis in normal rat GCs treated with FSH (3.3 nM) and variable hCG and 2-NBDG for 4h. (E) Glycogen content in the ovaries of immature rats treated with only FSH (8 IU), FSH (8 IU) + hCG (10 IU), and only hCG (10 IU). Glycogen in ovaries was quantified by chemical method. (F) Inhibition of insulin-stimulated incorporation of D-[U-^{14}C]-glucose into glycogen in rat GCs treated with hCG. (G) hCG-mediated inhibition of the upregulation of IRS-2 expression by FSH in normal rat GCs. Total RNA was subjected to qPCR with IRS-2 and β2M primers. The results are expressed as fold increase over basal. Data are presented as mean ± SEM (n = 3-5). *$p < 0.001$ vs. untreated, $^{\#}p < 0.001$ vs. FSH treated.

Fig. 6. Increased proximity of FSHR and LHR in the presence of both hCG and FSH. (A) The uptake of FSH-stimulated 2-NBDG was significantly inhibited in the presence of hCG. Histogram shows that at low concentrations (0.01-0.5 nM), hCG enhanced the FSH-stimulated glucose uptake ($p<0.05$). (B) With fixed hCG (3.3 nM) and variable FSH concentrations, the inhibition of glucose uptake caused by hCG was robust. (C) HEK293 cells expressing FLAG-LHR and HA-FSHR were incubated with increasing concentrations of FSH for 1h and then 2-NBDG for 30 minutes. Significant increase in 2-NBDG uptake was observed with FSH alone. (D) HEK293 cells expressing FLAG-LHR and HA-FSHR were treated with increasing concentrations of hCG for 1h and 2-NBDG for 30 minutes. Significant increase in 2-NBDG uptake was observed with hCG alone. Data are presented as mean ± SEM (n=6) *$p< 0.001$. (E) Increase in BRET signal w.r.t untreated cells in HEK293 cells co-expressing FSHR-Rluc8 and LHR-Venus after treatment with increasing concentration of FSH in the presence of constant hCG (3.3 nM). (F) Increase in BRET signal w.r.t untreated cells in HEK293 cells co-expressing FSHR-Rluc8 and LHR-Venus after treatment with varying concentration of hCG in the presence of constant FSH (3.3 nM). (G) FSH alone does not increase BRET signal in HEK293N cells expressing both FSHR-Rluc8 and LHR-Venus. (H) hCG alone does not increase BRET signal in HEK293N cells expressing both FSHR-Rluc8 and LHR-Venus. Results are expressed as area under the curve from 5 experiments (n = 5) and were analyzed by one way ANOVA, *$p< 0.001$.

Fig. 7. A schematic outline depicting the mechanism by which FSH and LH regulate the glucose uptake and glycogen synthesis in preovulatory GCs.

FSH increases glucose uptake and glycogen synthesis in the preovulatory GCs through IRS-2/Akt2/GS pathway. Decreased IRS-2 expression in PCOS GCs because of the interference of FSHR signaling by LH, may decrease glucose uptake and its storage as glycogen. This study suggests a novel mechanism by which FSH and LH cross-talk to regulate the glucose metabolism in preovulatory GCs. Depleted glycogen stores in GCs of PCOS women may impair the follicular growth and maturation. P: Phosphorylation.

Table 1: Efficiency (EC_{50}) and Efficacy (E_{max}) of FSH and hCG on glucose uptake and glycogen synthesis in rat preovulatory GCs. The E_{max} value is the maximal response in terms of glucose uptake or glycogen synthesis induced by FSH. The E_{max} value represented for hCG is relative to FSH. Statistical analyses were performed with unpaired t-test (*P < 0.001).

Responses	FSH			hCG		
	E_{max}	EC_{50}	n	E_{max}	EC_{50}	n
Glucose uptake	100%	0.92 ± 0.02 nM	5	51.55± 0.15%*	6.25 ± 0.03 nM*	6
Glycogen Synthesis	100%	3.18 ± 0.07 nM	6	13.80 ± 1.09%*	NA	4

Table 2: FSH-mediated increase in glucose uptake and glycogen synthesis in GCs of normal, PCOS-nonIR and PCOS-IR women.

Group	No. of subjects	Percentage of subjects with FSH-stimulated glucose uptake (FC >1.8; *p< 0.05*)	Percentage of subjects with FSH-stimulated glycogen synthesis (FC >1.8; *p< 0.05*)
Normal	34	100	100
PCOS-nonIR	19	46.12 ± 8.29	58.52 ± 20.16
PCOS-IR	22	18.24 ± 5.09	22.41± 2.50

FC, fold change; PCOS-nonIR, patients without insulin resistance; PCOS-IR, patients with insulin resistance

Table 3A: Inhibitory efficiency **(**IC_{50}) of hCG for FSH-stimulated glucose uptake and inhibitory efficiency **(**IC_{50}) of FSH for glucose uptake in hCG-treated HEK293 cells expressing both FSHR and LHR. The E_{max} value is the maximal response in terms of glucose uptake induced by FSH. The E_{max} value represented for hCG is relative to FSH. Statistical analyses were performed with unpaired t-test (*P < 0.001).

Response	hCG			FSH		
	E_{max} (FSH)	IC_{50}	n	E_{max} (hCG)	IC_{50}	n
Glucose uptake	100%	4.91 ± 0.01 nM	6	43.78 ± 0.57%*	0.15 ± 0.03 nM*	6

Table 3B: Efficiency (EC_{50}) and Efficacy (E_{max}) of FSH and hCG on glucose uptake in HEK293 cells expressing both FSHR and LHR. The E_{max} value is the maximal response in terms of glucose uptake induced by FSH. The E_{max} value represented for hCG is relative to FSH. Statistical analyses were performed with unpaired t-test (*P < 0.001).

Response	FSH			hCG		
	E_{max}	EC_{50}	n	E_{max}	EC_{50}	n
Glucose uptake	100%	1.47 ± 0.02 nM	6	62.67 ± 0.60% *	1.41 ± 0.01 nM	6

Authors' role

NC and AG have contributed equally to the manuscript. Experiments other than BRET change were performed in the laboratory of RS by AG, NC, SK, RL, and AN. NM and MGD provided human samples and patient data. RS, KMD and TGS analysed the results. RS and FP did the BRET experiments. PC and ER coordinated the BRET investigations. RS designed the study, wrote the manuscript and contributed to the experiments. Coordination of the work outlined in the manuscript and supervision of the accuracy of the information was also done by RS. All authors critically read and approved the manuscript.

Highlights

- Gonadotropins have a direct role in glucose uptake, storage and utilization in preovulatory granulosa cells.
- FSH and not hCG upregulate the glycogen synthesis through IRS-2 pathway.
- PCOS patients with or without insulin resistance have impaired FSH-stimulated glucose uptake and glycogen synthesis.
- Attenuation of FSH-stimulated glucose uptake and storage results after co-treatments with FSH and hCG, *in vitro* as well as *in vivo*.
- Concurrent treatment with FSH and hCG increase the proximity of LHR to FSHR and is associated with defective glucose uptake and glycogen synthesis in HEK293 cells expressing both LHR and FSHR.

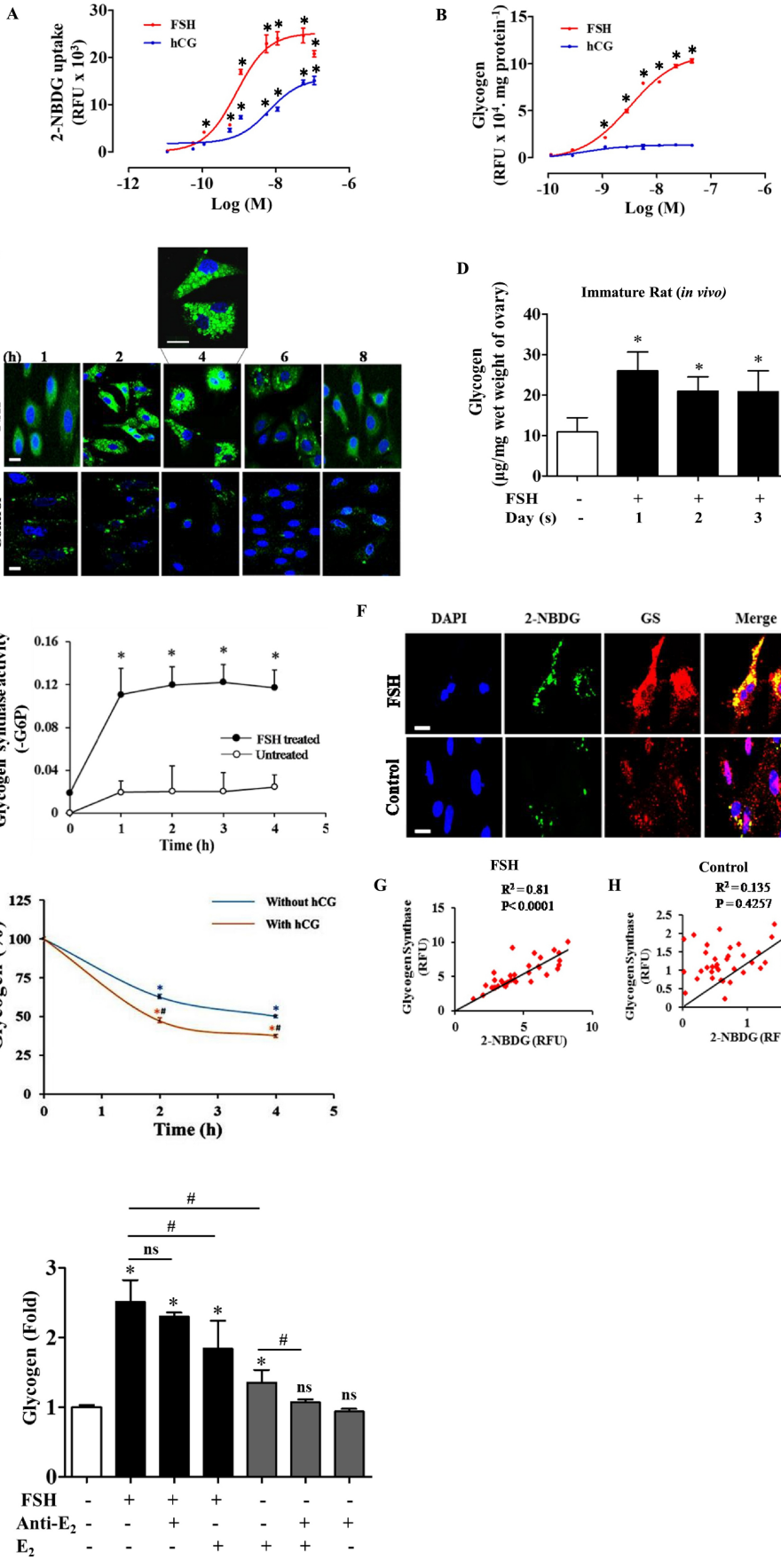
A
2-NBDG uptake (RFU x 10³)
FSH
hCG
Log (M)
B
Glycogen (RFU x 10⁴. mg protein⁻¹)
FSH
hCG
Log (M)
C
Time (h) 1 2 4 6 8
FSH
Control
D
Immature Rat (in vivo)
Glycogen (µg/mg wet weight of ovary)
FSH - + + +
Day (s) - 1 2 3
E
Glycogen synthase activity (-G6P)
FSH treated
Untreated
Time (h)
F
DAPI
2-NBDG
GS
Merge
FSH
Control
G
FSH
R²=0.81
P<0.0001
Glycogen Synthase (RFU)
2-NBDG (RFU)
H
Control
R²=0.135
P=0.4257
Glycogen Synthase (RFU)
2-NBDG (RFU)
I
Without hCG
With hCG
Glycogen (%)
Time (h)
J
Glycogen (Fold)
FSH - + + + - - -
Anti-E2 - - + - - + +
E2 - - - + + + -

Figure 1

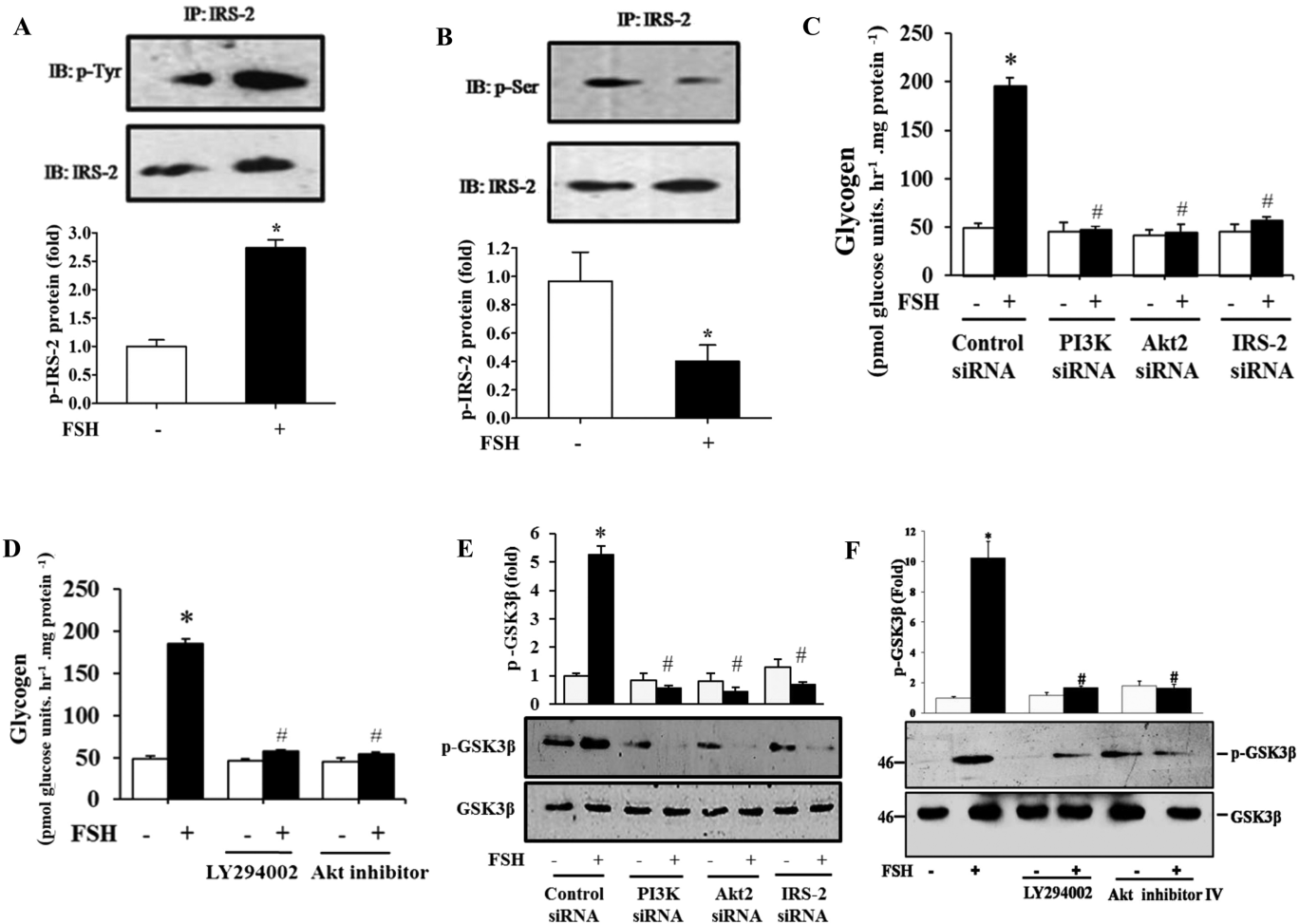
A
IP: IRS-2
IB: p-Tyr
IB: IRS-2
p-IRS-2 protein (fold)
FSH
B
IP: IRS-2
IB: p-Ser
IB: IRS-2
p-IRS-2 protein (fold)
FSH
C
Glycogen
(pmol glucose units. hr-1 .mg protein -1)
FSH
Control siRNA
PI3K siRNA
Akt2 siRNA
IRS-2 siRNA
D
Glycogen
(pmol glucose units. hr-1 .mg protein -1)
FSH
LY294002
Akt inhibitor
E
p -GSK3β (fold)
p-GSK3β
GSK3β
FSH
Control siRNA
PI3K siRNA
Akt2 siRNA
IRS-2 siRNA
F
p-GSK3β (Fold)
46
p-GSK3β
46
GSK3β
FSH
LY294002
Akt inhibitor IV

Figure 2

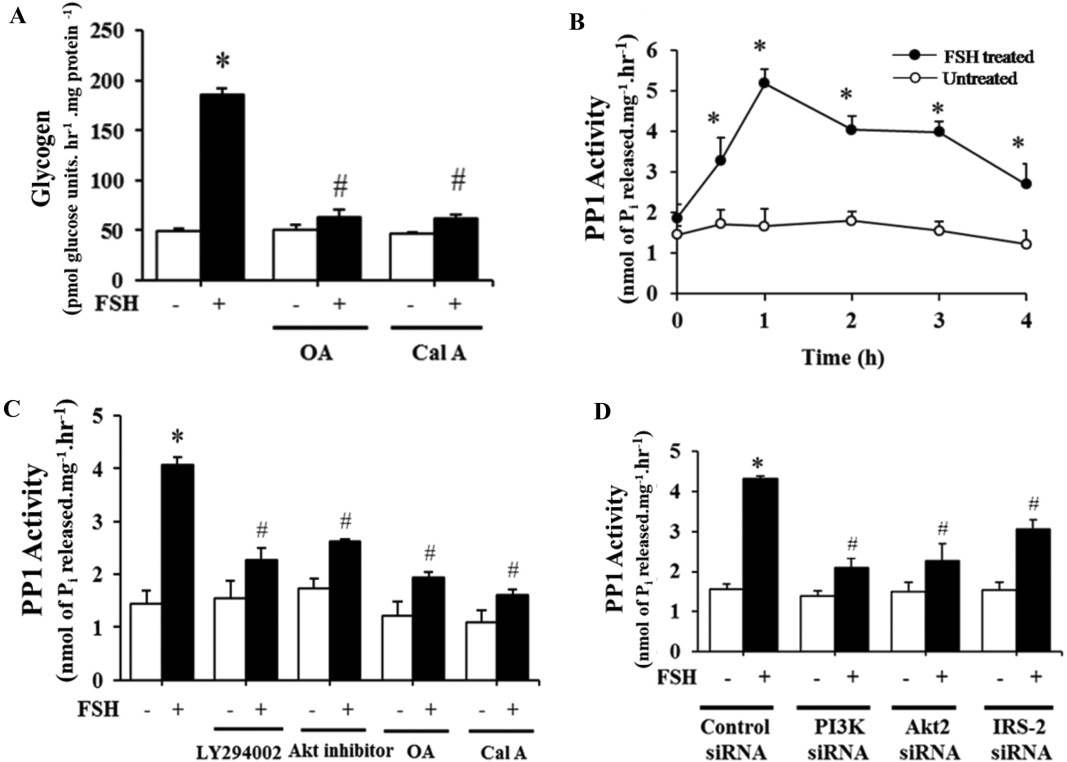
A
Glycogen
(pmol glucose units. hr-1 .mg protein -1)
250
200
150
100
50
0
FSH - + - + - +
OA
Cal A
B
PP1 Activity
(nmol of Pi released.mg-1.hr-1)
FSH treated
Untreated
Time (h)
C
PP1 Activity
(nmol of Pi released.mg-1.hr-1)
FSH - + - + - + - + - +
LY294002
Akt inhibitor
OA
Cal A
D
PP1 Activity
(nmol of Pi released.mg-1.hr-1)
FSH - + - + - + - +
Control siRNA
PI3K siRNA
Akt2 siRNA
IRS-2 siRNA

Figure 3

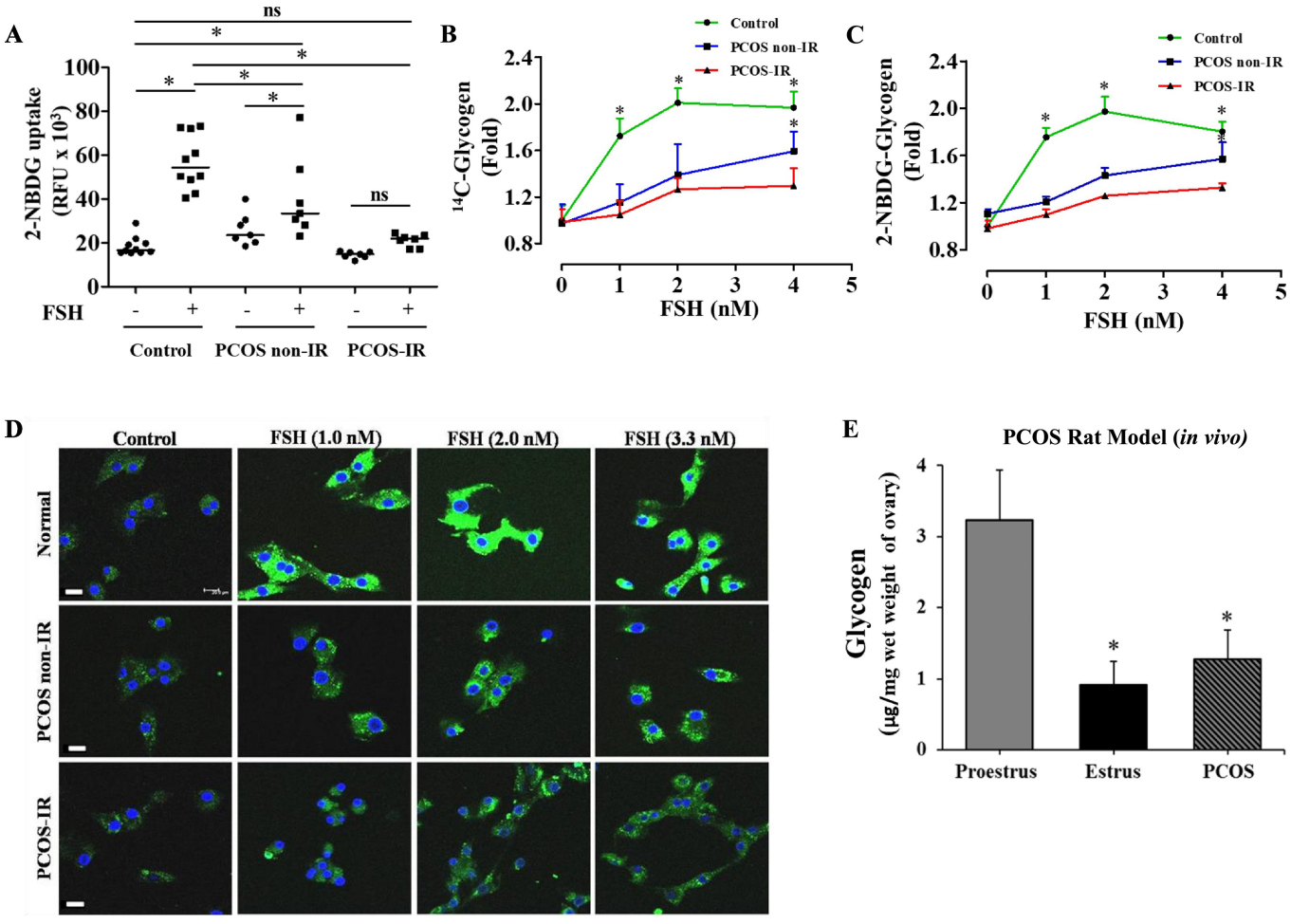
A
2-NBDG uptake (RFU x 10³)
ns
FSH
Control
PCOS non-IR
PCOS-IR
B
¹⁴C-Glycogen (Fold)
FSH (nM)
C
2-NBDG-Glycogen (Fold)
FSH (nM)
D
Control
FSH (1.0 nM)
FSH (2.0 nM)
FSH (3.3 nM)
Normal
PCOS non-IR
PCOS-IR
E
PCOS Rat Model (in vivo)
Glycogen (µg/mg wet weight of ovary)
Proestrus
Estrus
PCOS

Figure 4

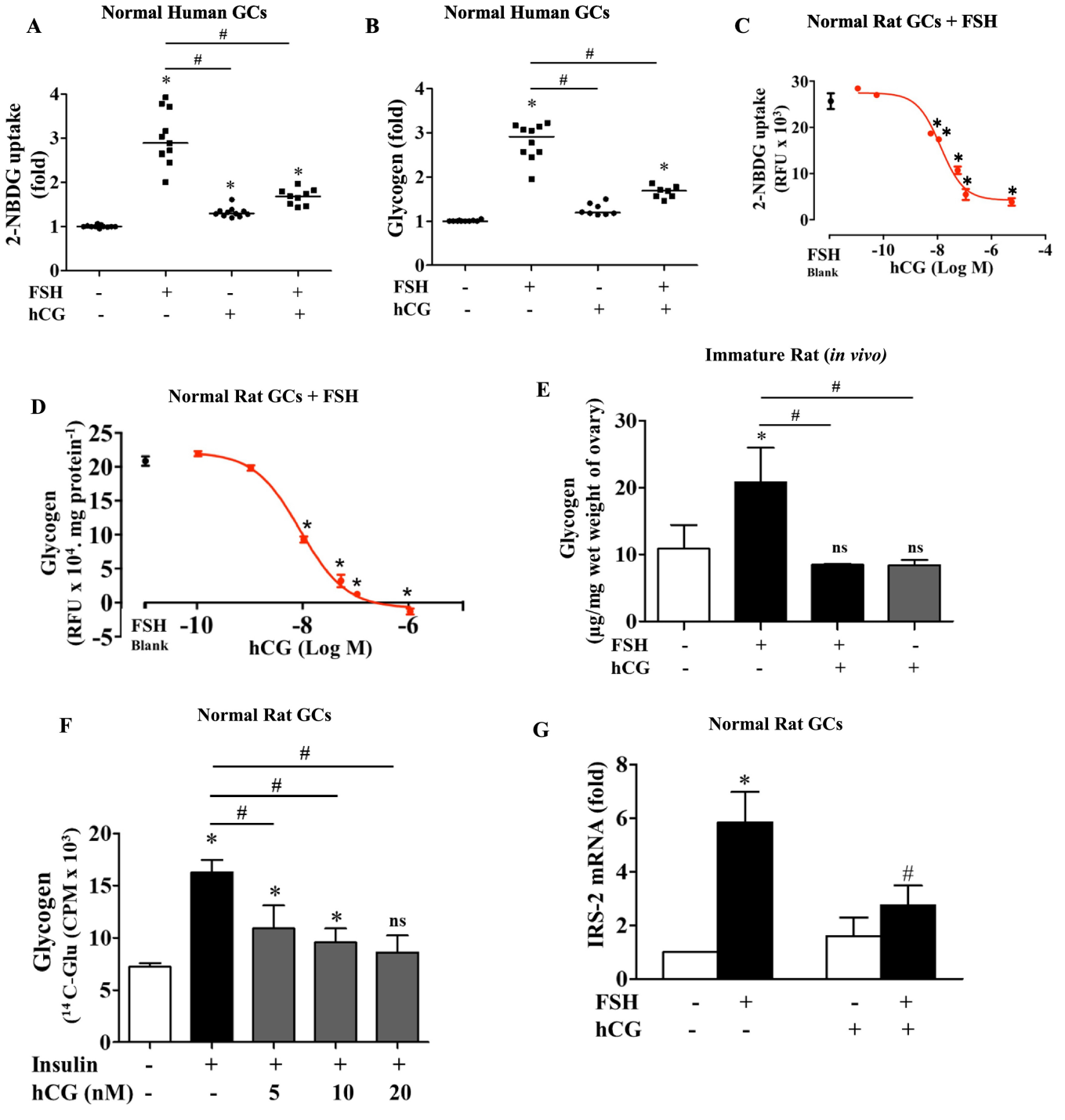
A
Normal Human GCs
2-NBDG uptake (fold)
FSH
hCG
B
Normal Human GCs
Glycogen (fold)
FSH
hCG
C
Normal Rat GCs + FSH
2-NBDG uptake (RFU x 10³)
FSH
Blank
hCG (Log M)
D
Normal Rat GCs + FSH
Glycogen (RFU x 10⁴. mg protein⁻¹)
FSH
Blank
hCG (Log M)
E
Immature Rat (in vivo)
Glycogen (µg/mg wet weight of ovary)
ns
FSH
hCG
F
Normal Rat GCs
Glycogen (¹⁴C-Glu (CPM x 10³)
ns
Insulin
hCG (nM)
G
Normal Rat GCs
IRS-2 mRNA (fold)
FSH
hCG

Figure 5

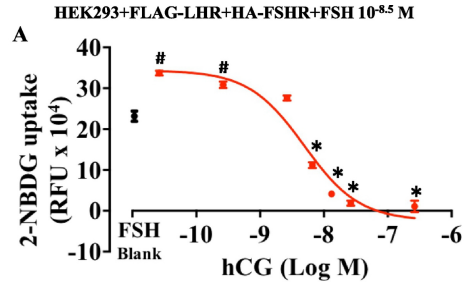
A
HEK293+FLAG-LHR+HA-FSHR+FSH 10-8.5 M
2-NBDG uptake (RFU x 10⁴)
FSH Blank
hCG (Log M)

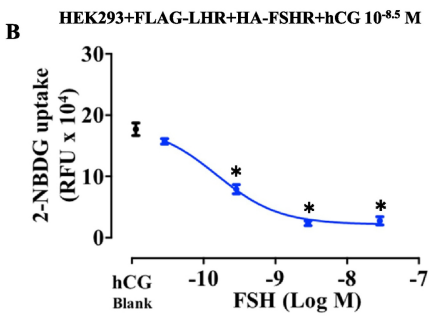
B
HEK293+FLAG-LHR+HA-FSHR+hCG 10-8.5 M
2-NBDG uptake (RFU x 10⁴)
hCG Blank
FSH (Log M)

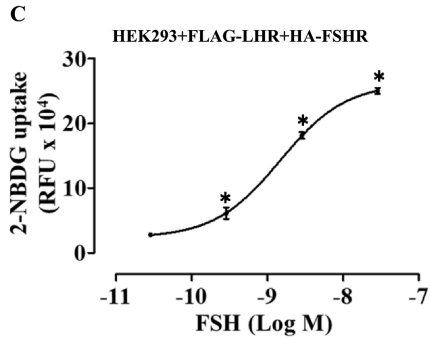
C
HEK293+FLAG-LHR+HA-FSHR
2-NBDG uptake (RFU x 10⁴)
FSH (Log M)

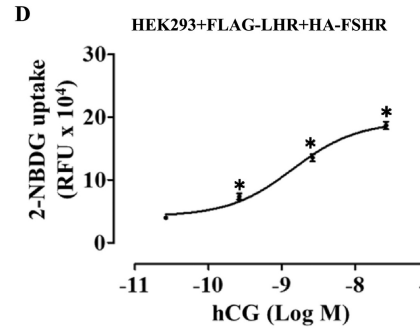
D
HEK293+FLAG-LHR+HA-FSHR
2-NBDG uptake (RFU x 10⁴)
hCG (Log M)

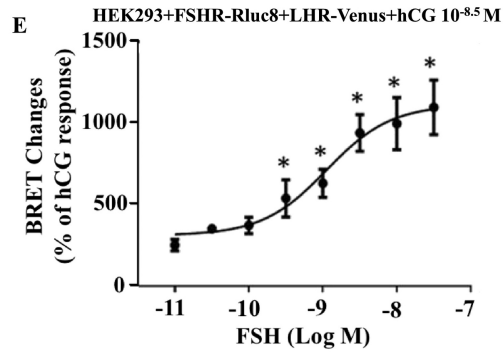
E
HEK293+FSHR-Rluc8+LHR-Venus+hCG 10-8.5 M
BRET Changes (% of hCG response)
FSH (Log M)

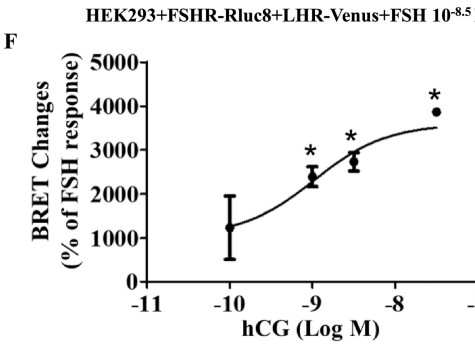
F
HEK293+FSHR-Rluc8+LHR-Venus+FSH 10-8.5 M
BRET Changes (% of FSH response)
hCG (Log M)

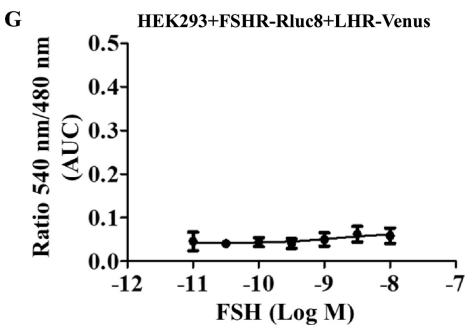
G
HEK293+FSHR-Rluc8+LHR-Venus
Ratio 540 nm/480 nm (AUC)
FSH (Log M)

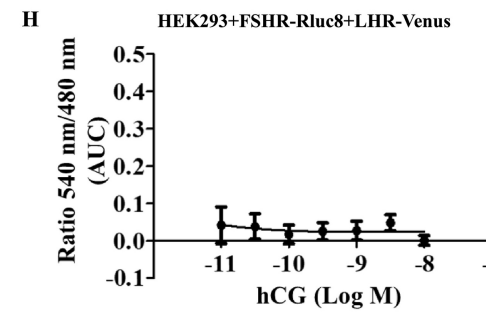
H
HEK293+FSHR-Rluc8+LHR-Venus
Ratio 540 nm/480 nm (AUC)
hCG (Log M)

Figure 6

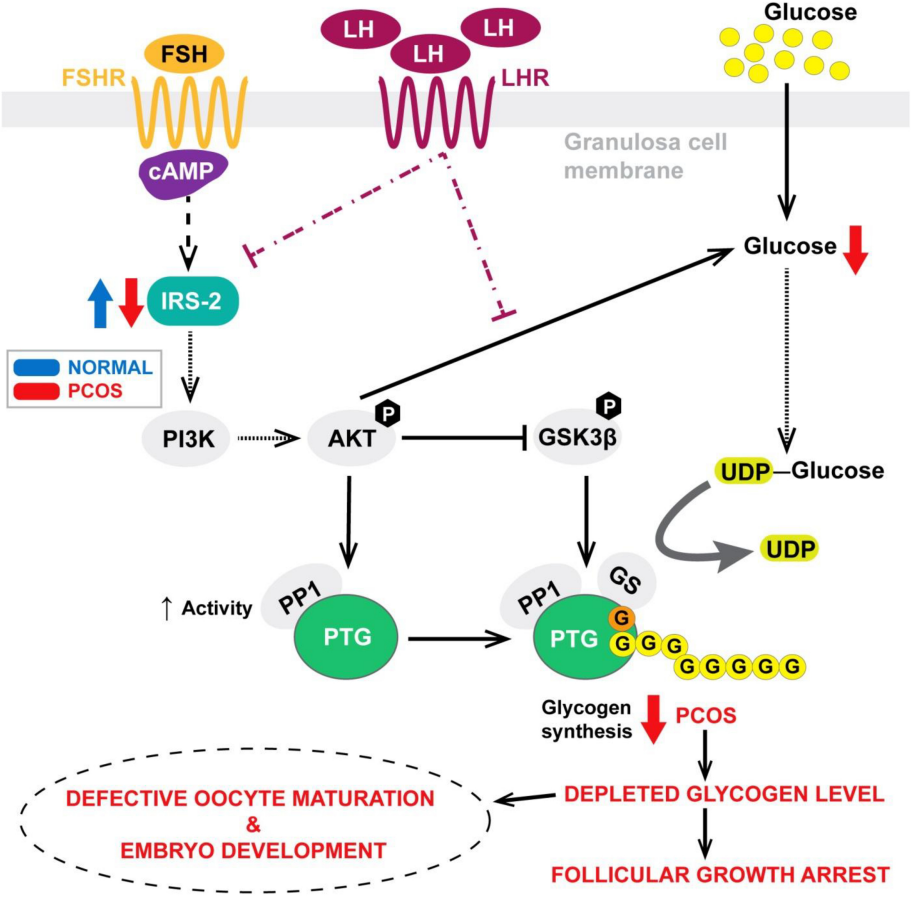
FSH
FSHR
cAMP
LH
LH
LH
LHR
Glucose
Granulosa cell membrane
Glucose
IRS-2
NORMAL
PCOS
PI3K
AKT
P
GSK3β
P
UDP—Glucose
UDP
↑ Activity
PP1
PTG
PP1
GS
PTG
G
G G G
G G G G G
Glycogen synthesis
PCOS
DEFECTIVE OOCYTE MATURATION & EMBRYO DEVELOPMENT
DEPLETED GLYCOGEN LEVEL
FOLLICULAR GROWTH ARREST

Figure 7